The Impact of Adipose Tissue Drainage on Glucose Homeostasis

Dissertation
zur
Erlangung der naturwissenschaftlichen Doktorwürde
(Dr. sc. nat)

vorgelegt der
Mathematisch-naturwissenschaftlichen Fakultät
der
Universität Zürich
von

Julia Rytka
von
Deutschland

Promotionskomitee:

PD Dr. Daniel Konrad
Prof. Dr. Carsten A. Wagner
Prof. Dr. Marc Donath
Prof. Dr. Thomas A. Lutz
Prof. Dr. Emanuel Christ

Zürich, 2010

Erklärung

Diese Dissertation wurde von PD Dr. Daniel Konrad betreut. Sie wurde selbständig und ohne unerlaubte Hilfe angefertigt. Bei der Abfassung der Dissertation wurden im Sinne der Promotionsordnung der Mathematisch-naturwissenschaftlichen Fakultät der Universität Zürich vom 8. Juli 2002 keine anderen als die angegebenen Hilfsmittel verwendet.

Zürich, 25.8.10

1 Summary

Visceral obesity is an independent risk factor for the development of cardiovascular diseases and type 2 diabetes. This is likely due to inherent difference compared to subcutaneous fat (e.g. in cellular composition, adipokine release, etc.) and/or due to different venous drainage since secreted products such as adipocytokines and FFAs from subcutaneous fat are drained systemically into the vena cava, whereas secreted product from mesenteric or visceral fat are drained into the portal system. Exaggerated hepatic delivery of FFAs and pro-inflammatory cytokines originating from adipose tissue (and/or the gastrointestinal tract) result in hepatic insulin resistance and metabolic deterioration constituting "the portal theory".

The aim of this study was to determine the effects of excessive adipose tissue on whole-body glucose homeostasis depending on venous drainage of adipose tissue.

To obtain an artificial increase in adipose tissue mass, fat tissue transplantation was performed in mice. Epididymal fat pads of a donor mouse were stitched to the mesenterium of an acceptor mouse, thus, draining into portal vein simulating visceral fat accumulation. Alternatively, epididymal fat pads were stitched to the peritoneum of an acceptor mouse. In the latter model, fat transplants are drained systemically via vena cava. As controls, sham-operated littermates were analyzed.

Four weeks after transplantation glucose tolerance was determined by an intraperitoneal glucose tolerance test. Mice receiving systemic drained fat pads showed an improved glucose tolerance compared to sham-operated controls. In contrast, mice with portal transplanted fat pads showed an impaired glucose tolerance. Moreover, hepatic insulin resistance developed in portal-transplanted mice as assessed by a hyperinsulinemic-euglycemic clamp. In addition, insulin-stimulated Akt-phosphorylation was reduced in liver samples of portal-transplanted mice suggesting reduced hepatic insulin signalling. mRNA expression of Interleukin-6 (IL-6) was upregulated in portal-transplanted adipose tissue compared to the systemic-drained transplant. Furthermore, IL-6 concentration was increased in portal but not in systemic plasma samples of mice receiving a portal fat transplant. Intriguingly, wildtype mice receiving a portal fat transplant from IL-6 knockout mice showed normal glucose tolerance.

In conclusion, our results demonstrate that the metabolic fate of intra-abdominal fat tissue transplantation is determined by the delivery of inflammatory cytokines to the liver specifically via the portal system providing clear direct support for the portal hypothesis.

2 Zusammenfassung

Viszerale Adipositas ist ein unabhängiger Risikofaktor für die Entstehung kardiovaskulärer Erkrankungen und des Typ 2 Diabetes. Dieser Zusammenhang beruht wahrscheinlich einerseits auf intrinsischen Unterschieden zwischen viszeralem und subkutanem Fettgewebe (zelluläre Zusammensetzung, Produktion von Zytokinen und Adipokinen), andererseits auf einer unterschiedlichen venösen Drainage dieser Fettgewebe. Viszerales Fettgewebe wird von der Pfortader drainiert. Entsprechend wird bei einer vermehrten Freisetzung von Zytokinen und Fettsäuren aus dem viszeralen Fettgewebe (beispielsweise im Rahmen einer Adipositas) die Leber solchen Veränderung direkt ausgesetzt und es kann sich eine hepatische Insulinresistenz entwickeln.

Ziel dieser Arbeit war es, mittels Fetttransplantation an Mäusen die Auswirkungen von Fettgewebslokalisation und entsprechend venöser Drainage der Fettgewebe auf die Glukosehomöostase zu untersuchen.

Epididymales Fettgewebe wurde einer Donor-Maus entnommen und anschliessend entweder ans Mesenterium oder ans Peritoneum einer Akzeptor-Maus genäht. Im ersten Fall wird das Transplantat portal drainiert, im zweiten Fall caval/systemisch. Dadurch wurde einerseits eine Zunahme des viszeralen und daher portal drainierten Körperfettes und andererseits eine Zunahme des subkutanen und daher systemisch drainierten Körperfettes simuliert. Alle Transplantate waren nach fünf Wochen gut durchblutet und morphologisch unauffällig. Als Kontrolle dienten Mäuse, die zwar operiert wurden aber kein Transplantat erhielten (Sham).

Vier Wochen nach Transplantation zeigten Mäuse, die ein systemisch drainiertes Fetttransplantat erhielten, eine im Vergleich zu Sham-operierten Mäuse eine verbesserte Glukosetoleranz, während Mäuse mit einem portal drainierten Transplantat eine verschlechterte Toleranz aufwiesen. Zudem ergab eine hyperinsulinämische-euglykämische Clamp eine hepatische Insulinresistenz in portal transplantierten Mäusen. Auch fand sich eine verminderte insulin-induzierte Phosphorylierung von Akt in der Leber portal transplantierter Mäuse, vereinbar mit vermindertem hepatischen Insulinsignalling. mRNA Expression von Interleukin-6 (IL-6) war erhöht in portal transplantiertem verglichen mit systemisch transplantiertem Fettgewebe. Auch fand sich eine erhöhte IL-6 Konzentration in portalem aber nicht im sytemischem Plasma von portal transplantierten Mäusen. Insbesondere zeigten Wildtyp-Mäuse, welche ein portales Fett-Transplantat von IL-6 Knockoutmäusen erhielten, eine normale Glukosetoleranz auf.

Schlussfolgernd lässt sich sagen, dass die Lokalisation und Drainage von Fettgewebe den Glukosestoffwechsel beeinflusst, wobei vor allem die portale Drainage von viszeralem Fettgewebe an der Entstehung einer hepatischen Insulinresistenz entscheidend beteiligt zu sein scheint.

3 Abbreviations

ACS	Acyl-CoA Synthetase
ACOD	Acyl-CoA-Oxidase
Akt	v-akt murine thymoma viral oncogene (PKB)
ANOVA	Analysis of variance
cDNA	complementary Deoxyribonucleic acid
DAB	3,3′-diaminobenzidine tetrahydrochloride
dNTP	Deoxyribonucleotide triphosphate
DTT	Dithiotreitol
EGTA	Ethylene glycol tetraacetic acid
ELISA	Enzyme Linked Immunosorbent Assay
FFA	Free fatty acid
HE	Haematoxilin Eosin
IL-6	Interleukin 6
MEHA	3-methyl-N-Ethyl-N-(beta Hydroxyethyl)-Anilin
Min	Minutes
mRNA	Messenger Ribonucleic acid
PBS	Phosphate buffered saline
PMSF	Phenylmethylsulfonyl fluoride
SOCS-3	Suppressor of cytokine signaling 3
TNFα	Tumor necrosis factor alpha
WHO	World Health Organization

4 Introduction

4.1 Obesity

Obesity is one of the greatest public health challenges of the 21st century. It has reached epidemic proportions globally, with more than 1 billion adults being overweight – at least 300 million of them clinically obese (Fig. 1). The prevalence of obese children and adolescents increased dramatically, affecting about 10 % of all children worldwide (1). However, the obesity epidemic is not restricted to industrialized societies, as obesity is often coexisting and developing faster in developing countries. Societal changes and worldwide nutrition transition are driving the epidemic with increased consumption of more energy-dense, nutrient-poor foods with high levels of sugar and saturated fats combined with less physical activity.

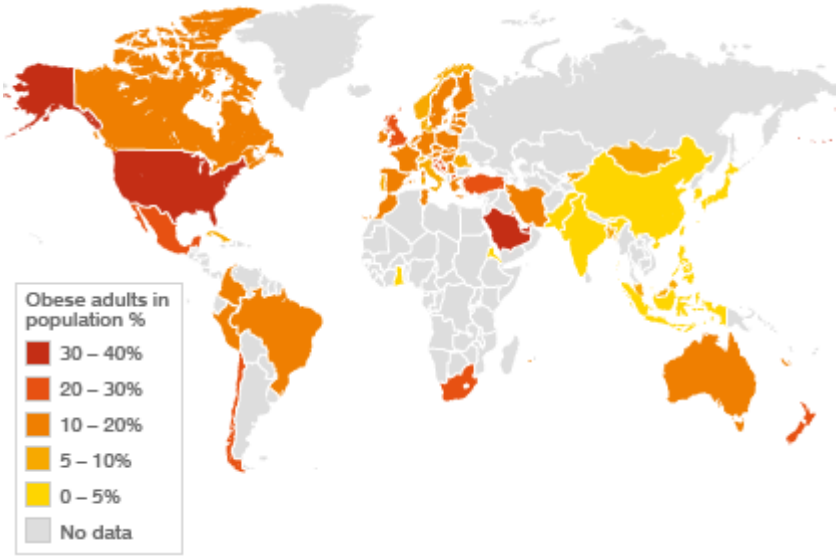

Fig 1: The global obesity problem (WHO, 2005)

Obesity (*from latin obesitas = fatness*) is defined as a condition where excessive accumulation of body fat becomes a severe nuisance to our health (and quality of life) and reduces life expectancy. The prevalence of overweight and obesity is commonly assessed by using body mass index (BMI), defined as the weight in kilograms divided by the square of the height in metres (kg/m^2). A BMI over 30 is defined as obese whereas a BMI over 40 means morbid obesity applying to both men and women and to all adult age groups (Table. 1). This

classification allows comparisons of weight status within and between populations and the identification of individuals and groups at risk of morbidity and mortality (2). Obesity causes or exacerbates many health problems. It is a major risk for serious diet-related chronic diseases, including type 2 diabetes, coronary heart diseases, certain forms of cancer, respiratory complications, and osteoarthritis of large and small joints. There is a close relationship between BMI and the incidence of several diseases, especially type 2 diabetes, wherein the risk is greatly increased for those subjects with a BMI above 29 (3).

BMI	WHO classification of BMI
< 16,5	= underweight
16,5 - 18,5	= meager
18,5 – 25	= normal
25 - 30	= overweight
30 - 35	= moderate obese or obese I
35 – 40	= severe obese or obese II
40 - 50	= morbid obese or obese III
> 50	= super obese

Table 1: WHO classification of BMI

4.2 Diabetes mellitus

Diabetes mellitus has reached epidemic proportions and affects more than 200 million people worldwide. Moreover, the prevalence of diabetes for all age groups worldwide is projected to be doubled in 2030 (4).

4.2.1 Definition of Diabetes mellitus

Diabetes mellitus is a chronic disease that occurs when the pancreas does not produce enough insulin or when the body cannot effectively use the insulin it produces. A common effect of uncontrolled diabetes is raised blood sugar that over time leads to damages of nerves and blood vessels. Generally, two types of diabetes mellitus are defined *(WHO, 2009)*:

- Type 1 diabetes (previously known as childhood-onset) is characterized by deficient insulin production and requires daily administration of insulin. Symptoms include excessive excretion of urine (polyuria), thirst (polydipsia), constant hunger, weight loss, vision changes and fatigue.
- Type 2 diabetes (also called adult-onset) is based on the body's ineffective use of insulin. It is largely the result of excessive body weight gain and physical inactivity. Approximately 85 % of people with diabetes are type 2, and of these, 90 % are overweight or obese. Until recently, this type of diabetes was confined to older adults but it is now also occurring in adolescents. Although lifestyle and overeating seem to be the triggering factors, genetic elements are also involved in the pathogenesis. The risk for type 2 diabetes has been calculated to be 38 % if one parent had this disease and is almost doubled if both parents are affected (5). Symptoms are similar to those of type 1 diabetes, but are often less marked. As a result, type 2 diabetes may be diagnosed several years after onset.
- Gestational diabetes is hyperglycaemia with onset or first recognition during pregnancy.

4.2.2 Obesity and type 2 diabetes

The likelihood of developing type 2 diabetes rises steeply with increasing body fatness. Increased body fatness is accompanied by profound changes in physiological functions, especially with regard to whole body glucose homeostasis. It is characterized by elevated fasting plasma insulin and an exaggerated insulin response to an oral glucose load. On the basis of WHO recommendations from 1999, there are diagnostic criteria for diabetes mellitus, incorporating both fasting and 2-h after glucose load orally (75 g). With a fasting plasma glucose concentration of more than 6.7 mmol/l or with more than 11.1 mmol/l after two hours of glucose load, a diabetes mellitus is classified. If plasma glucose concentrations are below 11.1 but above 7.8 mmol/l, an impaired glucose tolerance is diagnosed.

The mechanisms responsible for a normal glycaemia contain a balanced interplay between insulin secretion and insulin action. Insulin enhances glucose uptake by skeletal muscle, adipocytes and kidney cells and reduces glucose output by the liver. Therefore, hyperglycemia results either from decreased (absolute or relative) insulin secretion, e.g. due to beta cell dysfunction, or from reduced insulin action in target tissues, e.g. insulin resistance.

In addition, since insulin inhibits fatty acid release from adipose tissue, the lipolytic rate of adipose tissue is increasing causing elevated plasma levels of free fatty acids. In turn, the raised concentrations of glucose and fatty acids in the bloodstream will feed back to worsen both insulin secretion and insulin resistance. However, pancreatic beta cells often adapt to changes in insulin action. Between normal beta cell function and insulin sensitivity exist a curvilinear relation (6). Therefore, a decrease in insulin action is compensated by an upregulation of insulin secretion. Only in case of a deviation from this curvilinear relation, a deterioration of glucose tolerance will occur. In such patients, insulin secretion due to beta cell dysfunction is too low for a certain degree of insulin sensitivity/resistance.

4.2.3 Long-term consequences of diabetes

The risk of heart disease and stroke is increased in diabetic people: more than 50 % die of cardiovascular disease. In addition, longstanding diabetes may damage peripheral nerves (diabetic neuropathy) in more than half of the patients. Combined with reduced blood flow, neuropathy increases the chance of foot ulcers and eventually limb amputation. Diabetes is among the leading causes of kidney failure. 10 -20 % of diabetic people die of kidney failure. Long-term accumulated damage to the small blood vessels in the retina leads to diabetic retinopathy, the most important cause of acquired blindness in Western societies.

4.2.4 Treatment of type 2 diabetes – relation to disease mechanisms

The most efficient treatment remains weight reduction (diet, exercise, appetite modulators, and in severe forms bariatric surgery). Weight reduction leads in most patients to a profound improvement in glucose homeostasis. However, long-term weight reduction is often difficult to achieve. There are presently two main strategies to treat patients with overt type 2 diabetes in which weight reduction could not be achieved or was not sufficient: 1) increasing circulating insulin levels by either enhancing beta cell function or substitution with insulin, and/or 2) improving insulin sensitivity.

4.3 Insulin

4.3.1 Insulin synthesis and secretion

The hormone insulin is synthesized in β-cells of pancreatic islets. These islets have mainly endocrine functions and are named after its discoverer “islets of Langerhans”. Beside beta cells, they contain α-cells for glucagon secretion and δ-cells for somatostatin production. Furthermore, the pancreas has exocrine functions: it secretes digestive enzymes and bicarbonate into the intestinal lumen.

Insulin is generated from a proinsulin precursor molecule by the action of proteolytic enzymes which cleave the proinsulin at two sites, releasing the C-peptide (connecting peptide) and the mature insulin molecule. Insulin synthesis as well as the secretion of insulin from secretory granules, is stimulated by an increase in blood glucose concentration. Insulin and C-peptide are released into the portal vein. Approximately 60 % of all insulin is removed in the first liver passage. In contrast, C-peptide is not extracted by the liver at all so that C-peptide levels are often measured to determine whole insulin production.

4.3.2 Role of insulin

Insulin regulates the energy and glucose metabolism in the body by stimulating common anabolic pathways. Insulin stimulates glucose uptake into muscle, fat and kidney cells from circulation as well as its storage in form of glycogen in liver and muscle. In the liver, insulin has four major effects. First, it promotes glycogen synthesis by enhancing the transcription of glucokinase and by activating glycogen synthase. Insulin inhibits also glycogen breakdown to glucose by reducing the activity of glycogen phosphorylase and glucose-6-phosphotase. Second, insulin promotes glycolysis and carbohydrate oxidation by increasing the activity of glucokinase, phosphofructase and pyruvate kinase. By inhibiting the activity of phosphoenolpyruvate carboxykinase and glucose-6-phosphotase, insulin inhibits gluconeogenesis. Third, insulin promotes the synthesis and storage of triglycerides by increasing the activity of acetyl CoA carboxylase and fatty acid synthase. Additionally, fat oxidation is inhibited indirectly causing increased levels of free fatty acids for re-esterification to triglycerides and storage in lipid droplets. Fourth, insulin enhances protein synthesis.

In skeletal muscle, insulin promotes glycogen synthesis from glucose by enhancing the transcription of hexokinase and by activating glycogen synthase. Most notably, glucose uptake is increased through recruitment of GLUT4 transporters to the plasma membrane. The increased activity of hexokinase, phosphofructokinase and pyruvate dehydrogenase enhances glycolysis and carbohydrate oxidation.

In adipocytes, insulin promotes uptake of glucose and its conversion to triglycerides for storage. To this end, recruitment of GLUT4 transporters is promoted. In addition, enhancement of glycolysis leads to the formation of α-glycerol-phosphate which is esterified with free fatty acids to triglycerides. At the same time, insulin inhibits lipolysis by decreasing the activity of hormone sensitive triglyceride lipase to block the breakdown of triglycerides. Additionally, insulin promotes the conversion of pyruvate to free fatty acids by stimulating pyruvate dehydrogenase and acteyl CoA carboxylase. Free fatty acids are also released from triglycerides contained in chylomikrones and VLDL by insulin-stimulated lipoprotein lipase.

4.3.3 Insulin signalling and insulin resistance

Insulin signalling is initiated with the binding of insulin to its receptor, a tyrosine kinase receptor. Activation of the tyrosine kinase results in the addition of a phosphate molecule to particular tyrosine residues (phosphorylation) on "substrate" proteins such as the insulin receptor substrate 1 (IRS-1). SH-2 containing proteins (e.g. phospatidylinositol 3-kinase) dock onto certain phosphorylated tyrosine groups on the IRSs, and thus become activated. Activation of phosphatidyl inositol 3-kinase (PI-3-K) phosphorylates phosphatidyl inositol-4,5-biphosphate (PIP_2), to form phosphatidyl inositol-3,4,5-trisphosphate (PI-3,4,5-P_3), which in turn activates phosphatidyl inositol-dependent kinase (PDK). PDK is finally activating PKB activates the serine/threonine protein kinase Akt (also called protein kinase B, PKB) as well as the atypical protein kinase C isoforms λ and ζ which leads to the insertion of GLUT4 glucose transporters into the plasma membrane enhancing glucose uptake. In addition, PDK also phosphorylates and, thus, inactivates glycogen synthase kinase-3 (GSK-3). By inhibiting this kinase, glycogen synthesis is enhanced by insulin. Moreover, PDK activates mTOR (target of rapamycin), which promotes the translation of mRNA into protein. Moreover, activation of the insulin signaling pathway stimulates enzymes involved in lipid metabolism or the MAP kinase pathway being responsible for gene expression and growth.

In states of insulin resistance, insulin signaling may be negatively modulated on different levels. Inhibitory triggers, like inflammatory cytokines, adipokines as well as high glucose and non esterified fatty acids (NEFA) levels, affect their respective signal modulators and consequently inhibit propagation of the insulin signal. For example, the proinflammatory cytokine interleukin 6 enhances expression of SOCS-3, which in turn degrades IRS proteins (7).

4.4 Adipose tissue

The adipose tissue has a major role in the regulation of nutrient and energy homeostasis. In addition, it is involved in the modulation of immune responses, reproductive function, haemostasis, mechanical support, bone mass growth and thermogenesis. There are two types of adipose tissue depending on its cell structure, location, colour, vascularisation and function: white adipose tissue (WAT) and brown adipose tissue (BAT). WAT represents the vast majority of adipose tissue in the organism and is the site of energy storage, whereas BAT contains a large number of mitochondria and is specialized in heat production and energy expenditure (8) particularly in small mammals and human neonates.

Adipose tissue consists of a large number of adipocytes (the main cellular component), other non-fat cells, connective tissue matrix, vascular and neural tissues. The non-adipocyte cellular component includes inflammatory cells (macrophages), immune cells, preadipocytes and fibroblasts. Adipocytes constitute the main storage depots of the energy in form of triglycerides droplets. Conversely, they catabolise triglycerides in order to release glycerol and fatty acids that participate in glucose metabolism in liver and other tissues. As adipocytes grow larger (hypertrophic), they become dysfunctional and insulin resistant, resulting in an increased release of free fatty acids.

4.4.1 Adipose tissue as an endocrine organ

Adipose tissue is not only known for its capacity to store the excess of dietary intake as triglycerides. Furthermore, adipose tissue is the largest endocrine organ in the body, secreting adipokines (i.e. hormone-like factors released by the adipose tissue), cytokines and other proteins with specific biological functions. One of the best studied adipokine is leptin discovered in 1994. Leptin levels correlate directly with adipose tissue mass (9) and it

influences body weight, food intake, and fat stores via the hypothalamus. Leptin has been shown to modulate the activity of different subtypes of hypothalamic neurons bearing leptin receptors, thereby reducing food intake and increasing energy expenditure. In fact, mice with a mutation in the leptin (ob/ob mice) or leptin receptor (db/db mice) gene, as well as human subjects with mutations in the same genes, are massively obese (10). Another important adipokine is adiponectin which enhances insulin sensitivity. Moreover, it increases fatty acid oxidation in liver and skeletal muscle promoting lipid catabolism and decreasing triglyceride storage. In addition, it was reported to decrease the expression of adhesion molecules within the vascular wall, resulting in a decreased atherogenic risk. In humans, the role of the adipokine resistin is controversial whereas in mice it is known to induce glucose intolerance and insulin resistance. Probably it decreases the activity of AMP-activated protein kinase and increases the expression of gluconeogenic enzymes in the liver (8).

4.4.2 Adipose tissue as an initiator of inflammatory response

Obesity is associated with the recruitment of bone marrow-derived macrophages into adipose tissue. These adipose tissue macrophages (ATMs) are a major source of proinflammatory cytokines and chemokines, recruiting additional macrophages and propagating the chronic inflammatory state. Released proinflammatory cytokines including TNFα, IL-1β and IL-6 may profoundly alter adipocyte function resulting in altered secretion patterns of adipokines and cytokines as well as an increased release of free fatty acids. Consequently, insulin resistance may develop both locally, i.e. in adipose tissue, as well as systemically. Consistent with such notion, elevated levels of proinflammatory cytokines such as TNFα and IL-6 as well as of free fatty acids have been shown in individuals with insulin resistance and diabetes.

4.4.3 Distribution and localization of adipose tissue

Adipose tissue distribution may vary in obese people. In general, two different phenotypes of fat distribution are defined: increased accumulation of subcutaneous adipose tissue in the hip and thigh region (often referred as gynoid type or pear-shaped type of obesity) or increased accumulation of mainly visceral and upper thoracic adipose tissue (android type or apple-shaped type of obesity). Normally it does not exist only one phenotype, often one type is dominating. Especially the accumulation of visceral adipose tissue constitutes a

cardiovascular risk factor and is often associated with metabolic anomalies, like insulin resistance, arterial hypertension and dyslipidemia (11).

Visceral adipose tissue in humans include mesenteric as well as omental adipose tissue and is by definition drained to the portal vein whereas subcutaneous adipose tissue as well as perirenal adipose tissue is drained to the caval vein. As a consequence, factors released by portal drained adipose tissue, like FFAs, cytokines and adipokines are delivered directly into the liver where they are supposed to induce hepatic insulin resistance and/or steatosis. In rodents, a unique fat pad is found intra-abdominal closely located to the gonads (perigonadal or epididymal (in male mice) fat depot). This fat pad is drained to the vena cava inferior. An overview of different adipose tissue depots is shown in a mouse model (Fig. 2).

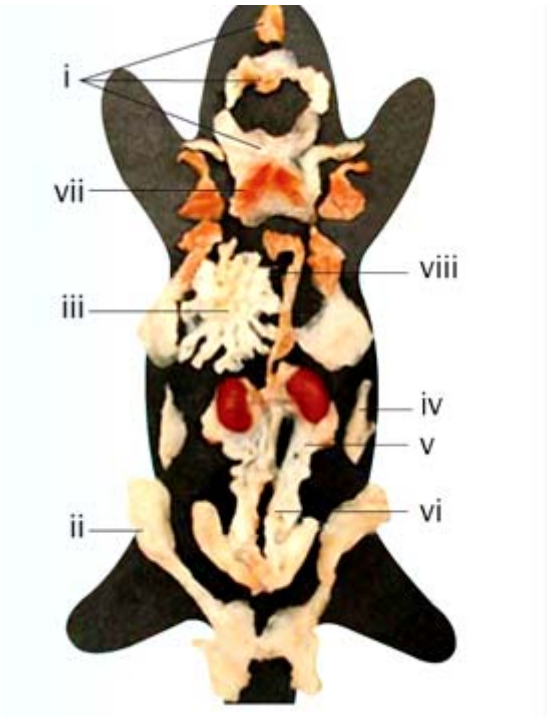

Subcutaneous white adipose tissue
i Anterior white adipose tissue
ii Inguinal adipose tissue

Intra-abdominal visceral white adipose tissue
iii Mesenteric adipose tissue
iv Retroperitoneal adipose tissue
v perinephric
vi perigonadal adipose tissue

Brown adipose tissue
vii interscapular brown adipose tissue
viii mediastinal adipose tissue

Fig. 2: The white subcutaneous, intra-abdominal visceral and brown adipose tissue depots are shown in a mouse model. Adapted from Murano, I. *et al*. *Adipocytes* 1, 121–130 (2005).

In the literature, intraabdominal adipose tissue is often used synonymously for visceral adipose tissue. However, as explained above, visceral adipose tissue in its proper sense includes only those intra-abdominal fat pads that are drained to the portal vein.

4.4.4 Characteristics of visceral and subcutaneous adipose tissue

Adipocytes from visceral adipose tissue (VAT) are morphologically and functionally different from subcutaneous adipose tissue (SAT). Fatty acid turnover and lipolysis are higher in visceral adipocytes and these cells are less responsive to the antilipolytic effect of insulin. Moreover, in contrast to subcutaneous fat cells, visceral fat cells express higher glucocorticoid receptor levels and respond to glucocorticoids with lipoprotein lipase activation (12). Among hormones secreted by adipocytes, leptin levels are more closely correlated with subcutaneous than with visceral fat.

There are also different aspects concerning proinflammatory cytokines, for example their expression levels in different fat depots (13). TNFα was shown to be involved in adipocyte metabolism by suppressing the expression of many adipose-specific genes, such as lipoprotein lipase, and by stimulating lipolysis, leading to decreased triglyceride accumulation in adipocytes. Expression levels of TNFα were often shown to be equal in VAT and SAT. However, it was shown that mRNA expression of the inflammatory cytokine Interleukin-6 is higher in VAT. IL-6 stimulates acute-phase proteins and activates the hypothalamus-pituitary-adrenal axis. IL-6 plasma levels are proportional to fat mass, whereas they are higher secreted from VAT than in SAT (14). In liver, IL-6 impairs insulin signalling through the induction of SOCS-3 expression and is often discussed to contribute to hepatic insulin resistance (15). The monocyte chemo-attractant protein-1 (MCP-1) has an essential role in the recruitment of macrophages to adipose tissue. In obese patients its expression is increased in adipose tissue when compared to lean individuals. Commonly, VAT is more infiltrated with inflammatory cells and is more capable of generating those proteins than SAT (16).

4.5 The portal theory associated with visceral fat accumulation

Visceral obesity has been often linked with insulin resistance, glucose intolerance, dyslipidemia, and cardiovascular disease. Especially, the liver has been implicated as a primary site for the development of insulin resistance associated with visceral obesity. As explained above, obesity is associated with increased release of proinflammatory cytokines and free fatty acids as well as altered production of adipokines. In the case of visceral obesity, the liver is directly exposed to these factors since they were released into the portal vein. As a consequence, hepatic insulin resistance as well as hepatic steatosis (lipid accumulation) occurs. Such hypothesis is often referred as the “portal hypothesis”. This means that chronic

exposure of the liver to elevated FFAs would promote liver gluconeogenesis, deplete enzymes involved in FFA oxidation, and increase hepatic lipogenesis (17). In addition, elevated FFA levels are known to increase liver triglyceride content and decrease insulin clearance, both of which are associated with insulin resistance. The higher lipolytic capacity in visceral adipocytes with its greater sensitivity to beta adrenergic stimulation and its lower sensitivity to the anti-lipolytic effect of insulin, enforce additional fatty acid flux to the liver (11). Moreover, different cytokines were shown to impact on hepatic insulin sensitivity. For instance, there are several studies supporting a role of IL-6 to inhibit insulin signalling in the liver (15, 18), likely through the induction of SOCS-3 expression leading to inhibition of IRS-1 activation (19-21).

5 Aims of the study

To determine the effects of excessive adipose tissue on whole-body glucose and energy homeostasis a novel fat tissue transplantation paradigm was used.

We hypothesized that beneficial and adverse effects of adipose tissue on whole-body glucose and energy homeostasis depend on venous drainage of adipose tissue, changes in adipokine/cytokine profile and alterations in food intake and/or energy expenditure.

6 Methods

6.1 Animals

Male C57BL6JOlaHsd mice were purchased from Harlan Netherlands (Horst, The Netherlands) and male IL-6 KO mice and their respective wild-type mice were from Charles River Laboratories (Wilmington, MA, USA). AFasKO mice were produced as described previously (21). All mice were housed in a pathogen-free environment on a 12-h light-dark cycle, with free access to standard rodent diet (Provimi Kliba, Kaiseraugst, Switzerland). All protocols conformed to the Swiss animal protection laws and were approved by the Cantonal Veterinary Office in Zurich, Switzerland.

6.2 Surgical procedure for portal and caval transplantation

Transplantation procedure was performed at 6 weeks of age. Mice were anaesthetized with isoflurane (Abbott, Baar, Switzerland). Both epididymal fat pads were removed from the donor mouse, weight and rinsed with 0.9% saline. Both pads were stitched to the visceral side of the peritoneum (caval transplantation) or to the mesenterium of the recipient mouse (portal transplantation) using Monocryl 6.0 (Johnson-Johnson, Spreitenbach, Switzerland). At the end of surgery, peritoneum was closed with Vicryl 5.0 (Johnson-Johnson, Spreitenbach, Switzerland) and the skin was stapled (3M Health Care, Neuss, Germany). Sham-operated control mice received the same treatment, but instead of the fat pad transplantation, an artificial suture was performed with Vicryl 5.0. Subcutaneous injection of buprenorphine every 12 h for 2 days was used for analgesia. In order to prevent transplant rejection, donor and recipient mice were littermates.

6.3 Hyperinsulinemic-euglycemic clamps

The hyperinsulinemic-euglycemic clamp technique is presently the “gold standard” for measuring insulin sensitivity in vivo. During clamping, insulin is infused via a catheter intravenously to raise the insulin concentration to supraphysiological levels. At the same time,

glucose is infused to maintain blood glucose at euglycemic levels (5-6 mmol/l; "clamping" of blood glucose levels) (22).

Seven days before clamping, mice are anesthetized with isofluran and a catheter (MRE 025, Braintree Scientific, Braintree, MA, USA) is inserted into the left jugular vein and exteriorized at the back of the neck. Upon recovery, only mice that have regained > 90 % of their preoperative weight are studied. After a fasting period of five hours, 3-[^{3}H] glucose (^{3}H-G) (0.1µCi/min; PerkinElmer, Schwerzenbach, Switzerland) is infused for 80 min and a blood sample is collected from the tail tip for basal turnover calculation. After basal sampling, insulin (18 mU/kg x min) is infused for 90 min. Euglycemia is maintained by periodically adjusting a variable infusion of 20 % glucose with a syringe pump (TSE systems, Bad Homburg, Germany). The glucose infusion rate is calculated as the mean of the steady state infusion which reached after about 60 min of insulin and glucose infusion (Fig. 3). A blood sample is collected after steady state infusion. The glucose turnover rate is calculated by dividing the rate of ^{3}H-G infusion by the plasma ^{3}H-G specific activity. Hepatic glucose production is calculated by subtracting the glucose infusion rate from the glucose turnover rate (23).

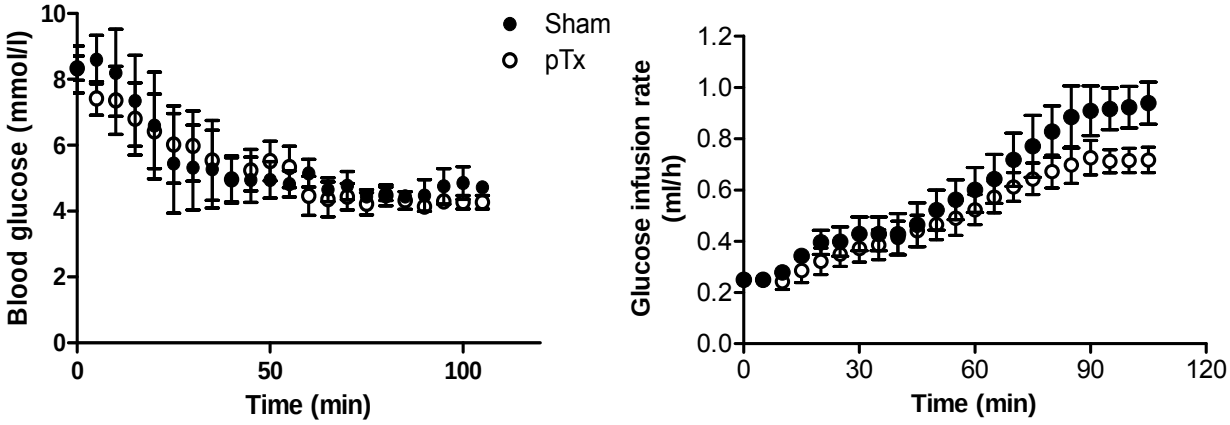

Fig. 3: Blood glucose concentrations and glucose infusion rate during hyperinsulinemic-euglycemic clamp. After a prime infusion of 3-[3H]-glucose for 80 min, insulin and 3-[3H]-glucose are infused via catheter into jugular vein (time point 0 min). Left graph: Blood glucose levels during a hyperinsulinemic-euglycemic clamp of Sham operated (○) and mice receiving portal drained fat pads (●). Blood glucose levels were clamped upon insulin infusion between 5 and 6 mmol/l. Right graph: To maintain euglycemia, increasing amounts of glucose needs to be infused. Glucose infusion rates increase until a "steady state" infusion is reached after about 60 min. Steady state glucose infusion is calculated as the mean infusion rate between 60 and 90 min.

6.4 Glucose tolerance tests

For the intraperitoneal glucose tolerance test (ipGTT) mice were fasted overnight (12 hours). Glucose (2g/kg body weight) was injected intraperitoneally and blood was collected from the tail vein at 0, 15, 30, 45, 60, 90 and 120 min after glucose administration (24). Plasma glucose was measured using a glucose meter (Ascensia Contour; Bayer, Zurich, Switzerland).

6.5 Insulin tolerance tests

For the intraperitoneal insulin tolerance test (ipITT) mice were fasted for fed and then fasted for three hours. Human normal insulin (0.75 U/kg body weight) were injected intraperitoneally and blood was collected from the tail vein at 0, 15, 30, 45, 60, 90 and 120 min after insulin administration.

6.6 Analyses of plasma samples

6.6.1 Determination of IL-6 in systemic and portal plasma

Systemic blood was collected by aspirating blood from the heart and for portal blood the portal vein was punctured after 3-5 h of fasting. Blood was centrifuged immediately with 8000 rpm for 10 min. Plasma IL-6 levels were determined with mouse LINCOplex kits from Linco Research, Inc. (Labodia, Yens, Switzerland). The kit is based on Luminex xMAPtechnology (Linco Research, St Charles, MI, USA) and use microsphere bead sets that are uniquely labelled with a mixture of two fluorescent dyes. The captured antibodies specific for each analyte are covalently coupled to individual bead sets. At the time of the assay, a mixture of beads is incubated overnight at 4°C with 10 µl of standards or mouse plasma samples in a 96-well filterbottom plate. On the next day, the beads are washed, and biotinylated detection antibody cocktail is added and incubated for 30 min at room temperature, followed by the addition of streptavidin-phycoerythrin and incubation for another 30 min. After a final wash, the resuspended beads are read on a Luminex 100 reader (Bio-Rad Laboratories, Hercules, CA, USA) and the concentration of each analyte in the samples to be tested is determined on the basis of individual standard curves.

6.6.2 Determination of plasma leptin and adiponectin

Blood samples were obtained from the tail vein of mice after overnight fasting.
Concentration of leptin and adiponectin was determined with mouse LINCOplex kits from Linco Research, Inc. (Labodia, Yens, Switzerland).

6.6.3 Determination of Non Esterified Fatty Acid (NEFA) in plasma samples

Systemic blood was collected by aspirating blood from the heart and for portal blood the portal vein was punctured after 3-5 h of fasting. Blood was centrifuged immediately with 8000 rpm for 10 min. NEFA levels were measured using the ACS-ACOD-MEHA method (Wako Chemicals GmbH, Neuss, Germany).

6.6.4 Determination of plasma insulin

Plasma was collected from the tail vein of mice after overnight fasting. Insulin was determined using an ELISA kit (Ultra Sensitive Rat Insulin ELISA; Crystal Chem, Downers Grove, IL, USA).

6.7 Total liver lipid extraction

Liver tissue (30mg) was homogenized in PBS and lipids were extracted in a chloroform-methanol (2:1) mixture. Total liver lipids were determined by a sulfphosphovanillin reaction as described by (25).

6.8 RNA extraction and quantitative reverse transcription-PCR (RT-PCR)

Total RNA from fat pads respectively liver tissue was extracted with the RNeasy lipid tissue mini kit (Qiagen). First strand cDNA synthesis was performed using Superscript III Reverse Transcriptase and random hexamer primer. Typically 0.75 µg of total RNA, 0.1 µl of random hexamer primer and 1 µl dNTPs (10mM) were adjusted with water to 13 µl and incubated at 65°C for 5 min in order to dissolve secondary structures of the RNA. After incubation on ice

for 1 min, 4 µl 5x first strand buffer, 1 µl 0.1M DTT, 1 µl RNase inhibitor and 1 µl Superscript III Reverse Transcriptase were (all reagents from Invitrogen, Basel, Switzerland) added to 13 µl reaction mix. Incubation circle started with 25°C for 5 min, followed by 50°C for 60 min and 70°C for 15 min. At the end, cDNA samples were stored at -80°C.

Taqman system (Applied Biosystems) was used for real-time PCR amplification. The cDNA samples were diluted 1/5 and 18S RNA (Applied Biosystems) for negative control was diluted 1/10 in water. Samples were loaded on a 96-well reaction plate (MicroAmp, Applied Biosystems, USA) containing 10 µl Universal PCR Mastermix (Taqman, Apllied Biosystems, USA), 1 µl of specific primer or 18S RNA, 7 µl water and 2 µl of diluted cDNA. The detection of the amplification was performed with the 7500 Fast Real-Time PCR System (Applied Biosystems, USA). Relative gene expression was obtained after normalization to 18sRNA, using the formula $2^{-\Delta\Delta cp}$ (26). The following primers were used: TNF-α Mm00443258_m1, IL-6 Mm00446190_m1, KC Mm00433859_m1, IL-1β Mm0043422/8_m1, MCP-1 Mm00441242_m1, Fas Mm00433237_m1, FasL Mm00438864_m1, cd11c Mm00498698_m1, Hif-1α Mm00468869_m1, SOCS3 Mm 00545913_s1, CD68 Mm03047343_m1, F4/80 Mm00802529_m1, cd11b Mm00434455_m1 (Applied Biosystems).

6.9 Western Blot

Tissue samples were pulverized in liquid nitrogen and homogenized in a buffer containing 150 mM NaCl, 50mM Tris-HCl (pH 7.5), 1mM EGTA, 1% NP-40, 0.25% sodium deoxycholate, 1mM sodium vanadate, 1mM NaF, 10mM sodium β-glycerophosphate, 100nM okadaic acid, 0.2mM PMSF and a 1:1000 dilution protease inhibitor cocktail (Sigma). Protein concentration was determined using conventional bicinchoninic acid (BCA) protein assay kit (Pierce, Rockford, USA) and equivalent amounts of protein (20-50µg) were resolved by LDS-PAGE (4-12% gel; NuPAGE, Invitrogen). Proteins were transferred to a nitrocellulose membrane (0.2µm, BioRad) and blocked for one hour in 5% non fat dry milk (BioRad) resolved in Tris buffered saline, containing 1% Tween 20. Membranes were incubated over night at 4°C on a rocking platform with respective primary antibodies. The following primary antibodies were used: anti-phospho-Akt (S473) and anti-Akt (Cell Signaling). Subsequently, membranes were incubated with secondary antibody (horseradish peroxidase-conjugated; Santa Cruz Biotechnology, and Alexis Biochemicals) for 1 hour at room temperature. Bands

were detected after 5 minute incubation with Lumi-Light substrate (Roche). Membranes were exposed in an Image Reader and analyzed with Image Analyzer (FujiFilm).

6.10 Histology

Five weeks after transplantation liver tissue was fixed in 4% buffered formalin and imbedded in paraffin. Tissue sections (4 µm) were deparaffinised with xylol (two times 10 minutes), rehydrated with 100, 95, 70 % ethanol (5 minutes each) and rinsed with dest. water. Sections were stained with haematoxylin for 10 minutes, washed and then put very shortly in ethanol/HCl. After washing for 10 minutes, sections were stained with Eosin (1 min). Sections were washed again and then shortly put in 70, 95, 100% ethanol and finally two times in xylol. Sections were mounted with Pertex (*Histo*-Lab, Goteborg, Sweden). Pictures were taken with Axioplan 2 microscope (Zeiss) and Axio Vision software (Carl Zeiss Image) with a 20x magnification.

Fat tissues were fixed in 4% buffered formalin and imbedded in paraffin. Sections were obtained either at the time of sacrification and stained with Hematoxylin/Eosin. For each fat pad of a mouse at least 100 adipocytes were analyzed. Images were analyzed using ImageJ software for quantification (National Institutes of Health, Bethesda, MD). Macrophage number was determined by Immunohistochemistry. For this fat tissue sections were deparaffinised and then given for 30 min in 0.3 % H_2O_2 in methanol. Sections were washed in PBS and incubated in normal serum to reduce non-specific background staining. Sections were incubated with the mac2 antibody (Cedarlane, Ontario, Canada) overnight at 4°C. After washing with PBS, sections were incubated with biotinylated secondary antibody for 30 min at room temperature. Sections were washed again and then incubated with ABC complex (ABC Kit Vectostain, Vector laboratories, Burlingame, USA). After washing, DAB (Zymed laboratories, Invitrogen, Carlsbad, USA) was used for histoenzymatic visualization. Mac2 positive cells were counted per nuclei of seven randomly selected fields per section containing at least 90 cells.

6.11 Indirect calorimetry, physical activity and ingestive behavior

For energy expenditure (EE) and respiratory quotient (RQ) determination, mice were individually housed in plexiglass air-tight cages designed for open circuit calorimetry

(AccuScan Inc., Columbus, OH, USA). Group sizes were: sham (n=5), systemic drainage (n=5), and portal drainage (n=6). Using Integra ME 2.21 software (AccuScan, Inc.), oxygen and carbon dioxide levels in each chamber were measured for 30 seconds every 5 minutes. Based on these values, EE and RQ were calculated according to (27) and used to determine average hourly and light- and dark-phase EE and RQ. The system simultaneously measured physical activity and food and water intake. For metabolic cages, mice were fed a standard powder chow containing 3.2 kcal/g (3433, Provimi Kliba AG, Kaiseraugst, Switzerland). Horizontal activity was determined by number of breaks in infrared photobeams that cross the cage in a 2D grid. For food and water intake measurements, each cage was equipped with a food hopper and water bottle placed on a scale that continuously monitored mass to the nearest 0.01g. Data were collected for four 22-hour days. Data from each animal was averaged over the four days to calculate representative values for each mouse used for statistical analysis.

6.12 Data analysis

Data are presented as means +/- SEM and were analyzed by Student's *t* test or analysis of variance (ANOVA) with a Turkey correction for multiple group comparisons respectively Bonferroni's post-hoc test for individual comparisons. A p-value < 0.5 was considered statistically significant. The software in use was Prism Version 5.0 (GraphPad Software Inc., San Diego, CA, USA).

7 Results

7.1 The impact of fat tissue localization and its venous drainage on glucose homeostasis

To estimate the potential metabolic effects of an artificial increase in fat tissue mass epididymal fat pads of a regular chow-fed donor mouse were transplanted to the peritoneum, resulting in systemically (via vena cava) drained transplants, or to the mesenterium, resulting in portally drained transplants, of a chow-fed littermate mouse. At the time of sacrifice (five weeks after transplantation), transplanted fat pads were adherent and well vascularised (Fig. 3A). Sham operation as outlined above was performed in control littermates. Mice tolerated the surgical procedure and the fat transplantation well - no adverse events were noted. In order to confirm venous drainage of transplanted fat pads to the portal vein, Evans Blue was injected retrogradely into the portal vein. As depicted in Fig. 3B, transplanted fat pads were stained with Evans Blue as was endogenous mesenteric fat tissue, but not caval-drained epididymal fat tissue, confirming the portal drainage of the mesenteric-transplanted fat tissue.

A

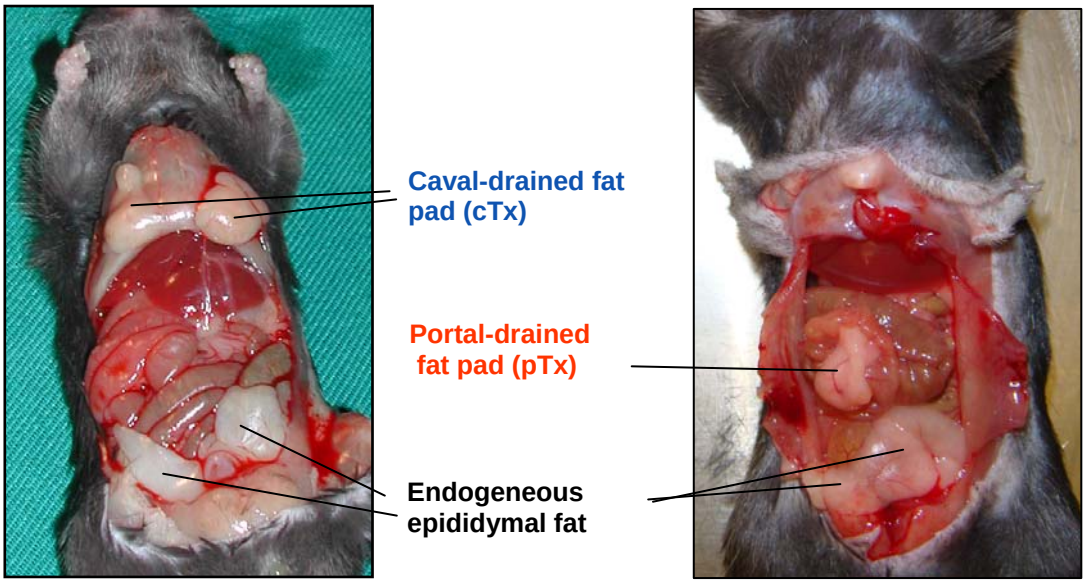

B

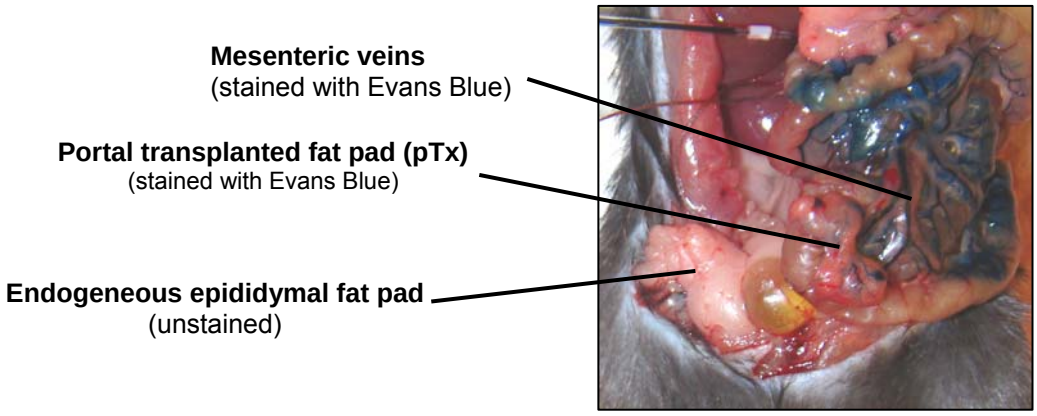

Fig. 3: Transplantation was performed at 6 weeks of age. Both epididymal fat pads were removed from a donor mouse and stitched to the peritoneum (cTx; left panel) or mesenterium (pTx; right panel) of a littermate recipient. **(A)** Six weeks after transplantation, the abdominal cavity was opened and the transplanted fat pad was visualized. **(B)** To confirm portal drainage of transplanted fat pads, Evans Blue dye (5mg/ml) was injected into the portal vein.

We have previously shown that mice receiving fat pads drained to the inferior vena cava had improved glucose tolerance (24). Four weeks after transplantation, body weight gain was not different between sham-operated mice and mice receiving a portal-drained fat transplant (3.0±0.4 g vs. 2.9±0.5 g; p=0.85). However, as depicted in Fig. 4A, increase in blood glucose concentrations after an intraperitoneal glucose load was significantly higher in mice receiving a fat transplant drained to the portal vein (portal-drained fat pad transplantation; pTx) compared to mice receiving caval-drained fat pad transplantation (cTx) as well as to sham-operated mice, indicating impaired glucose tolerance in mice receiving a portal drained fat pad transplant (Fig. 4A). To examine the potential role whether the transplantation procedure on its own deteriorates glucose homeostasis, for example, by altering the delivery of inflammatory mediators from the GI-tract, peritoneal tissue containing no adipocytes was transplanted to the mesenterium. As depicted in Fig. 4B, glucose tolerance was not impaired in such transplanted mice (Fig. 4B).

A

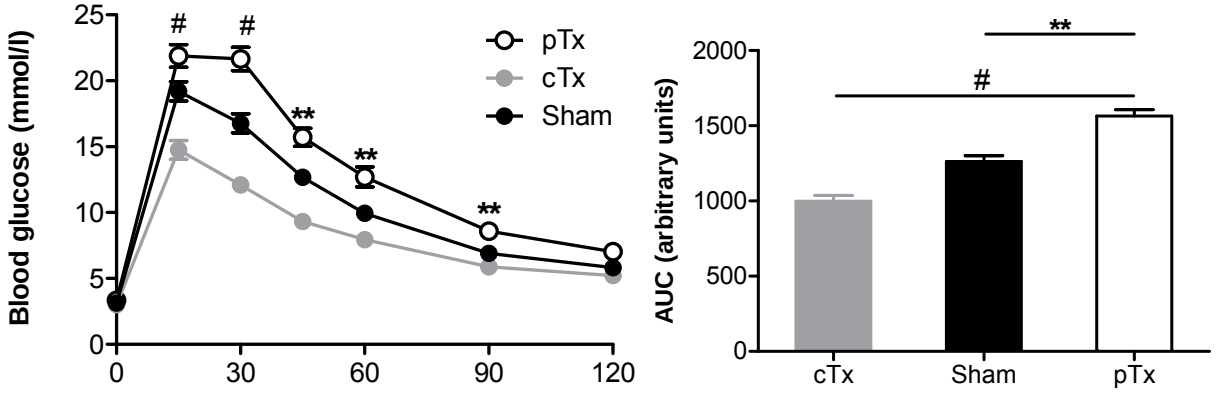

B

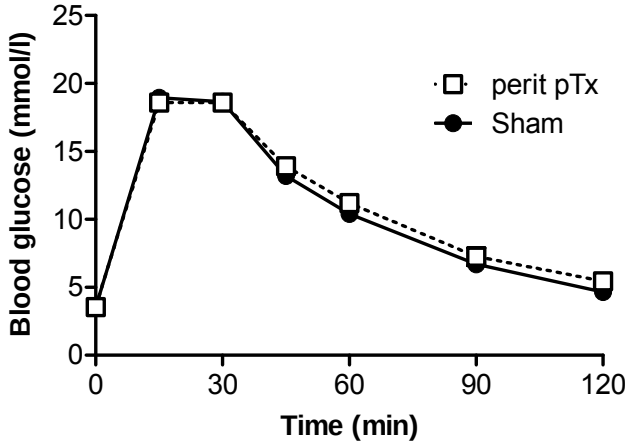

Fig. 4: Intraperitoneal glucose tolerance test (2 g glucose/kg body weight) was performed four weeks after surgical procedure in mice receiving portal drained transplants (pTx; ○), in mice receiving caval drained transplants (cTx; ●) or in sham-operated mice (●) after a overnight fast. Results are expressed as mean blood glucose concentration (left panel) or area under curve (right panel) ± SEM of 5 (pTx), 15 (cTx) or 25 (Sham) animals. **p < 0.01, #p < 0.001 (ANOVA). (B) Intraperitoneal glucose tolerance test (2 g glucose/kg body weight) was performed four weeks after surgical procedure in mice receiving portal drained peritoneal tissue transplants (perit pTx; □) or in sham-operated mice (●) after a overnight fast. Results are expressed as mean blood glucose concentration ± SEM of 2 animals.

To determine whether the effect on glucose homeostasis of one transplantation site predominates over the other, a double transplantation approach was performed, i.e. one epididymal fat pad of the donor mouse was stitched to the peritoneum (and, thus, drained to the inferior caval vein), the other pad was stitched to the mesenterium (and, thus, drained to portal vein). Transplanted fat pads were similar in size and originated from the same donor

mouse, which was a littermate of the recipient mouse. As depicted in Fig. 5 glucose tolerance in such transplanted mice was not different form sham-operated mice four weeks after surgery.

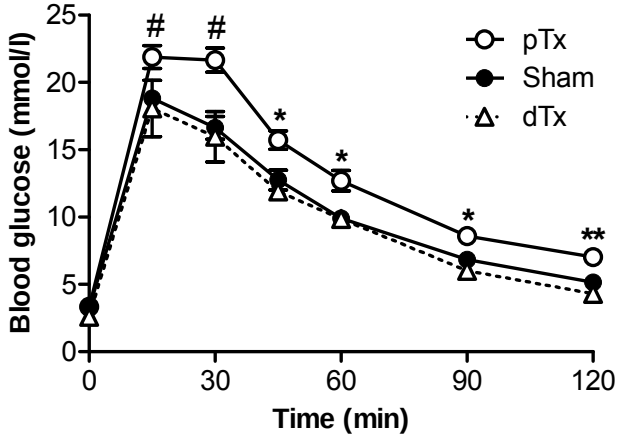

Fig. 5: Both epididymal fat pads were removed from a donor mouse. One was stitched to the peritoneum and the other to the mesenterium of the same littermate (dTx). Intraperitoneal glucose tolerance test (2 g glucose/kg body weight) was performed four weeks after surgical procedure in mice receiving a double transplant (dTx; Δ), in mice receiving a portal-drained transplant (pTx) or in sham-operated mice (●) after a overnight fast. Results are expressed as mean blood glucose concentration ± SEM of 3-8 animals.

We next assessed adipose tissue morphology of endogenous and transplanted fat pads in sham-operated and portal transplanted (pTx) mice. Adipocytes in portal transplanted fat pads were similar in size as endogenous mesenteric adipocytes but smaller than endogenous epididymal adipocytes (Fig. 6A, B). In addition, macrophage infiltration rate was much higher in portal transplanted compared to endogenous fat pads and sham-operated endogenous epididymal fat pads (Fig. 6C).

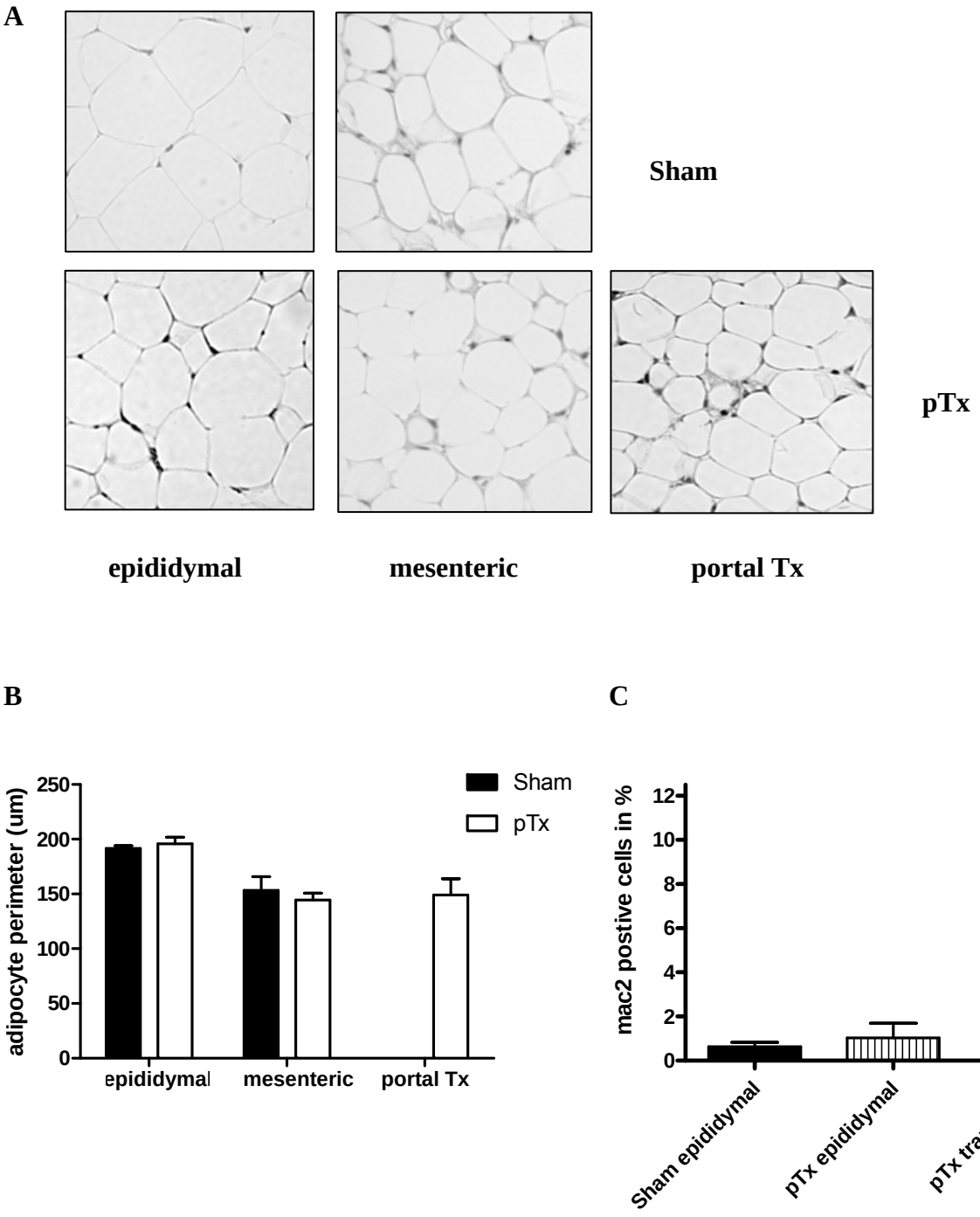

Fig. 6: (**A**) Representative, Hematoxylin and Eosin-stained histological sections of endogenous epididymal, endogenous mesenteric or transplanted fat pads from sham-operated mice and pTx mice are shown 5 weeks after transplantation. Adipocyte cell perimeter was measured using ImageJ. (**B**) Up to 100 cells for each fat pad were analysed and the results represent the mean ± SEM of three or four different mice. All values are expressed relative to the adipocyte cell perimeter of endogenous epididymidal fat pad of sham-operated mice. Black bar: sham-operated mice; white bar: mice receiving a portal fat transplant. (**C**) Histological sections of endogenous epididymal and portal transplanted tissue were immunostained with mac2 antibody. Mac2 positive cells were counted in seven randomly selected fields per section (about 90 cells) and expressed relative to total cell nucleus content. Results represent the mean ± SEM of four different mice.

Consistent with the portal theory, we hypothesized that portal-drainage of fat transplant would cause hepatic insulin resistance. To assess this possibility a hyperinsulinemic-euglycemic clamp was performed five weeks after surgery. Glucose infusion rate was significantly lower in portal transplanted mice compared to sham-operated mice (Fig. 7A and Fig. 3). Moreover, during hyperinsulinemic-euglycemic clamp, insulin-induced suppression of hepatic glucose production was blunted in mice receiving a portal-drained fat pad transplant, but was clearly evident in sham-operated mice (Fig. 7B). Therefore, mice receiving portal drained fat pad transplants drained to the portal vein developed hepatic insulin resistance. Furthermore, insulin-induced phosphorylation of Akt was markedly reduced in livers of portally transplanted mice compared to that of sham-operated mice (Fig. 7C, left panel). This eminent reduction in hepatic insulin signaling confirmed the development of hepatic insulin resistance in portally transplanted mice. In contrast, glucose disposal rate as well as insulin signaling in skeletal muscle were not affected by the portal-drained transplant (Fig. 7C, right panel), suggesting maintained insulin-sensitivity of skeletal muscle.

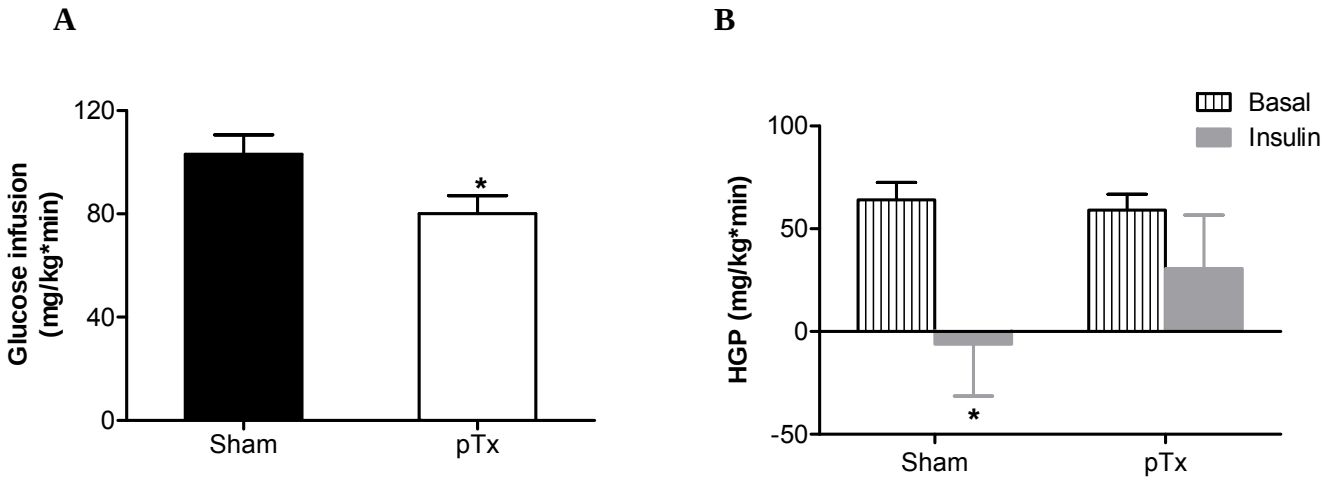

C

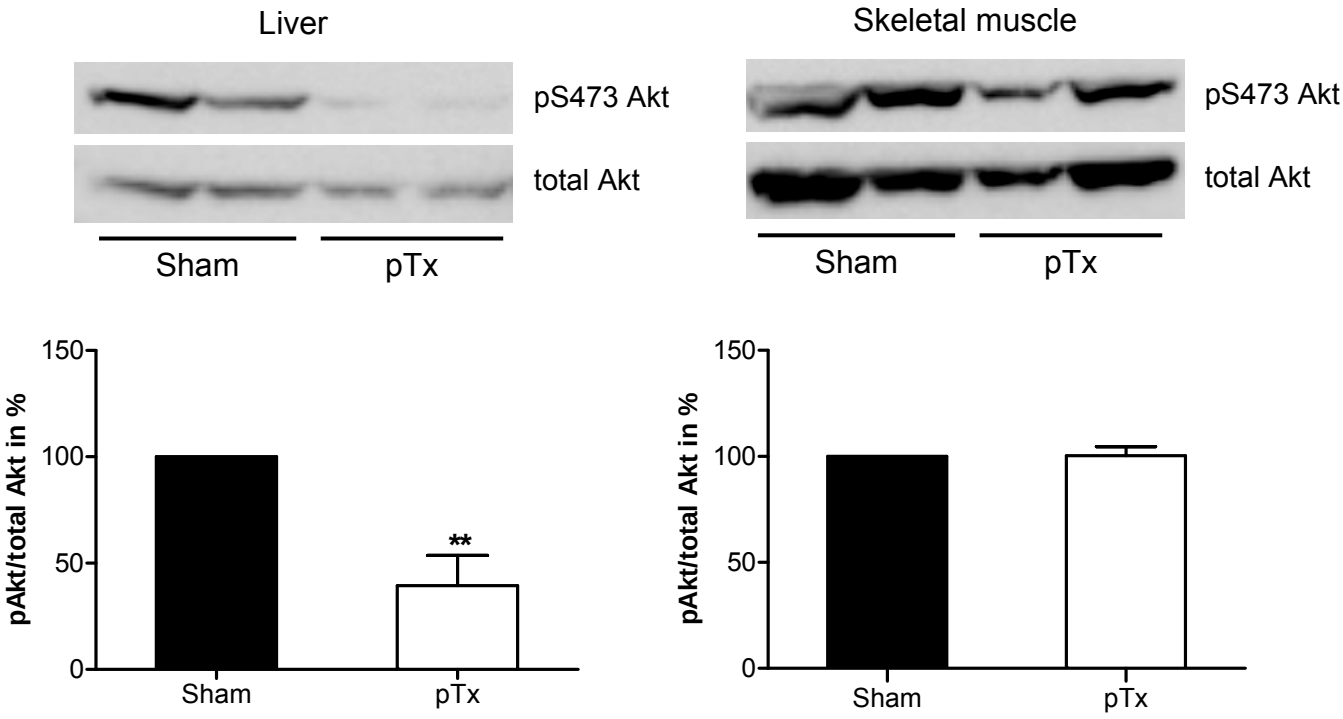

Fig. 7: Hyperinsulinemic-euglycemic clamps were performed 5 weeks after transplantation. (**A**) Glucose infusion rate was adjusted to a blood glucose level of 5 mM and kept constant for at least 20 min. (**B**) Hepatic glucose production (HGP) were calculated in the basal period and in response to insulin infusion (18 mU/kg/min) during the clamp study. Results are the mean ± SEM of 5 animals. *p < 0.05 (Student's *t* test). (**C**) Insulin (1U/kg) was injected i.p. in overnight fasted mice 5 weeks after transplantation. Liver and skeletal muscle samples were harvested 15 minutes later and phosphorylation of Akt at S473 was determined by Western blotting. A representative blot is shown in the upper panel. Results are the mean ± SEM of 3 animals. **p < 0.01 (Student's *t* test).

The development of hepatic insulin resistance is often associated with hepatic steatosis and Kupffer cell activation (28). Thus, hepatic lipid contents as well as expression levels of tissue macrophage markers were assessed. Histological examinations and biochemical determination of total hepatic lipid content was similar in sham-operated and portal transplanted mice (Fig. 8A/B). Moreover, no increased infiltration/activation of hepatic Kupffer cells was detected (Fig. 8C). Consistent with the absence of hepatic steatosis in portal transplanted mice, no differences in systemic and portal plasma free fatty acids (FFA) levels were found in both groups of mice (Fig. 8D). Thus, transplantation of fat pads to sites drained by the portal vein induces hepatic insulin resistance independently of hepatic steatosis and Kupffer cell infiltration/activation.

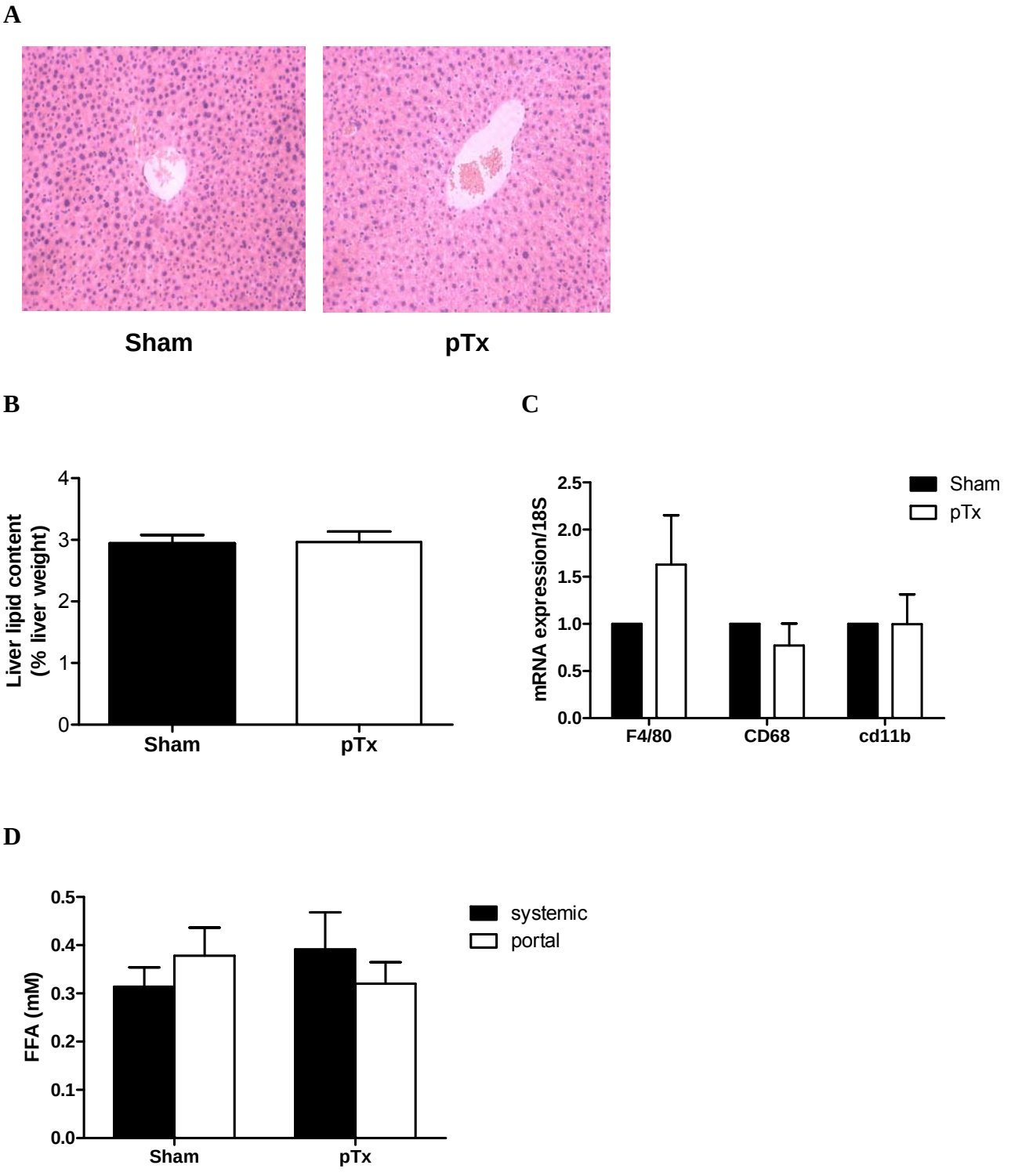

Fig. 8: (**A**) Hematoxylin and Eosin-stained liver sections from sham-operated and pTx mice. (**B**) Total liver lipids were determined and expressed relative to liver weight. Results represent the mean ± SEM of 4 to 6 mice of each group. (**C**) mRNA expression of indicated markers was analyzed in liver tissue of sham-operated and pTx mice. Results are the mean ± SEM of 5 mice per group, expressed relative to WT and normalized to expression of 18S. (**D**) FFA levels were determined in systemic and portal plasma samples of mice receiving a portal drained fat transplant (pTx) and in sham-operated mice after 3 hours of fasting. Results are the mean ± SEM of 5-6 animals.

To investigate potential mediators of hepatic insulin resistance observed in mice receiving portal-drained transplant. Transplanted fat tissue may not acquire the exact biological function as the endogenous fat tissue of the same depot, and its function may be affected by a combination of host and donor factors. Thus, to determine potential differences between caval and portal transplanted fat pads, we utilized endogenous and transplanted fat depots from the double transplanted mice. Such approach allowed us to exclude different host factors, as well as secondary metabolic effects induced by cTx versus pTx, as shown in Fig. 3. As depicted in Fig. 9A, transplanted fat tissue of either localization exhibited a much more inflammatory gene expression profile than endogenous epididymal fat pads, as assessed by mRNA expression of pro-inflammatory cytokines and cd11c. Yet intriguingly, when comparing portal transplanted to caval transplanted fat pads, the former exhibited higher expression levels of IL-6 and Fas ligand (FasL).

Since IL-6 was previously associated with hepatic insulin resistance (20-21) we postulated that increased IL-6 expression and secretion from portal transplanted fat pads might be responsible for hepatic insulin resistance. Thus, IL6 was determined in systemic and portal vein plasma samples of sham-operated and portal transplanted mice. Systemic and portal IL-6 plasma levels were similar in sham-operated mice, whereas IL-6 concentration was more than 70% higher in portal compared to systemic blood samples of mice receiving a portal drained fat transplant (Fig. 9B). Even though this difference was not significant these data suggest increased delivery of IL-6 to the liver of mice receiving a portal transplant, potentially originating from the transplanted fat pad. Consistent with an increased delivery of IL-6 to the liver, hepatic SOCS3 mRNA expression, which is induced by IL-6 (7), was enhanced in mice receiving a portal transplanted fat pad (Fig. 9C).

A

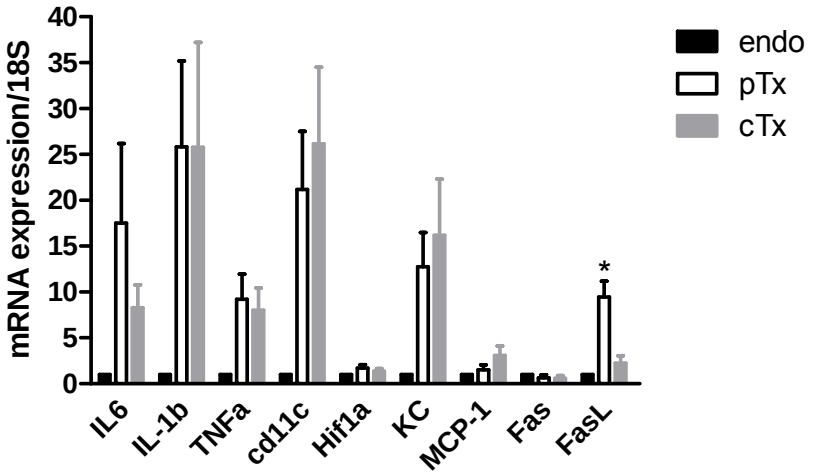

B

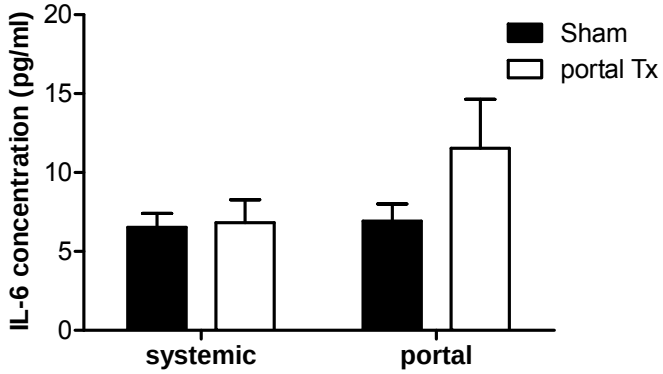

C

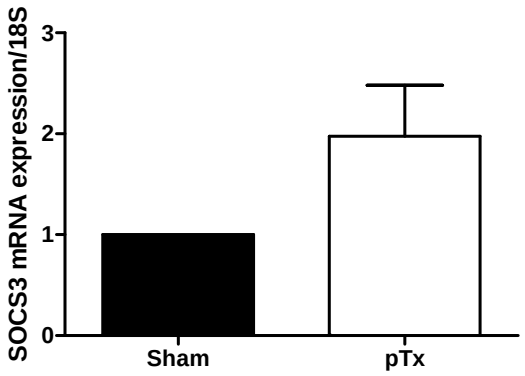

Fig. 9: (**A**) Five weeks after transplantation endogenous epididymal fat pads (endo), the portal-drained transplant (pTx) and the caval-drained transplant (cTx) were collected and rtPCR was performed. Results are the mean ± SEM of 3-7 animals. ** $p < 0.01$ pTx vs cTx (ANOVA). (**B**) IL-6 was measured in systemic and portal plasma samples of mice receiving a portal-drained fat transplant (pTx) and in sham operated mice. Results are the mean of ± SEM of 8-10 animals. (**C**) Five weeks after transplantation liver tissue was collected and rtPCR was performed. Results are the mean ± SEM of 5 animals.

To substantiate the potential contribution of IL-6 to the induction of insulin resistance in portal transplanted mice, epididymal fat pads of an IL-6 knockout donor were transplanted into a wildtype recipient (pTx-IL6KO). As shown in Fig. 10A, glucose tolerance of such transplanted mice was not impaired compared to sham-operated wildtype mice. Moreover, the insulin-induced increase in Akt-phosphorylation in liver samples was completely maintained in these mice (Fig. 10B) in contrast to mice receiving a portal-drained transplant from wildtype mice (Fig. 4). These results point towards a causative role for IL-6 in the development of insulin resistance in portal transplanted mice. The mRNA expression levels of proinflammatory cytokines were strongly downregulated in portal-transplanted IL-6 deficient fat pads compared to portal-transplanted fat pads of wildtype mice (Fig. 10C). This

suggests a common regulatory effect of IL-6 on other proinflammatory cytokines. Additionally, hepatic mRNA expression of SOCS-3 of portal transplanted mice, receiving IL6 deficient fat pads, was no longer enhanced as it was shown for mice receiving a transplant from wildtype mice (Fig. 10D).

A

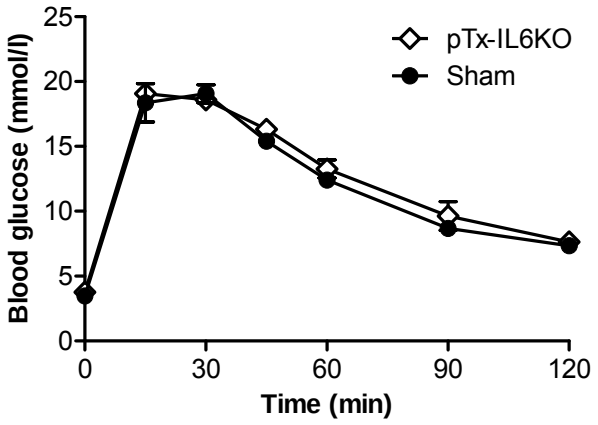

B

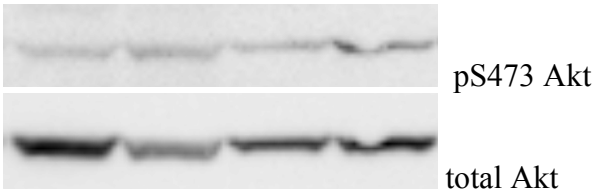

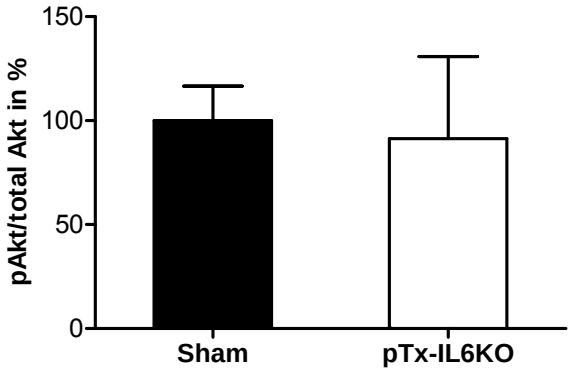

C

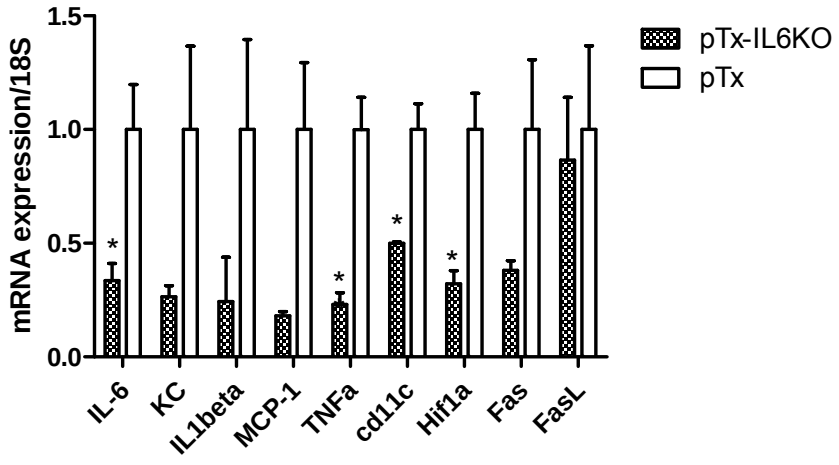

D

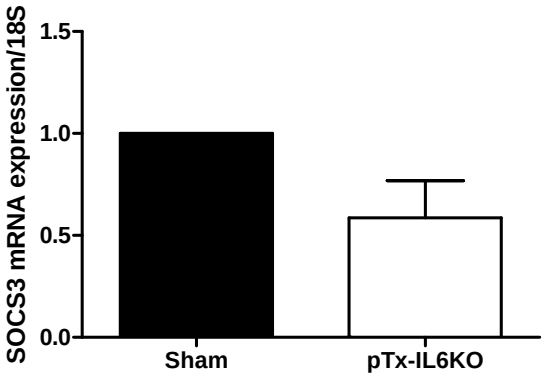

Fig. 10: Both epididymal fat pads were removed from an IL6-knockout mouse (donor) and stitched to the mesenterium of a wildtype mouse (recipient; pTx-IL6KO). (**A**) Intraperitoneal glucose tolerance test (2 g glucose/kg body weight) was performed four weeks after surgical procedure in mice receiving portal transplants (pTx-IL6KO; ◊) or in sham-operated mice (●). (**B**) Insulin (1U/kg) was injected i.p. in overnight fasted mice 5 weeks after transplantation. Liver and muscle samples were harvested 15 minutes later and phosphorylation of Akt at S473 was determined by Western blotting. A representative blot is shown in the upper panel. (**C**) Five weeks after transplantation, portal-transplanted fat pads of wildtype donor (pTx) and IL6-KO donor mice (pTxIL6-KO) were collected and rtPCR was performed. Results are the mean of ± SEM of 3 animals *$p<0.05$ (**D**) Five weeks after transplantation, liver of pTx-IL6KO mice was collected and rtPCR was performed. Results are the mean of ± SEM of 3 animals.

As shown in Figure 9A, mRNA expression of FasL was significantly higher in portal-transplanted compared to caval-transplanted fat pads. Such result suggests increased Fas activation in portal transplanted fat pad, which may induce secretion of proinflammatory cytokines such as IL-6. To estimate whether Fas activation contributes to the declined glucose homeostasis, epididymal fat pads of an adipocyte-specific Fas-knockout (AFasKO) mouse were transplanted portally to wildtype mice. It was shown by Wueest *et al*., that mice lacking Fas in adipocytes showed less adipose tissue inflammation and were partly protected from deterioration in glucose homeostasis induced by high-fat diet. Interestingly, mice receiving a Fas-deficient fat transplant showed normal glucose tolerance similar to sham-operated littermates (Fig. 11A). As expected and documented in Fig 11B, Fas was decreased in Fas-deficient fat transplants, but not in endogenous epididymal fat tissue of transplanted and sham-operated mice (Fig.11B).

A

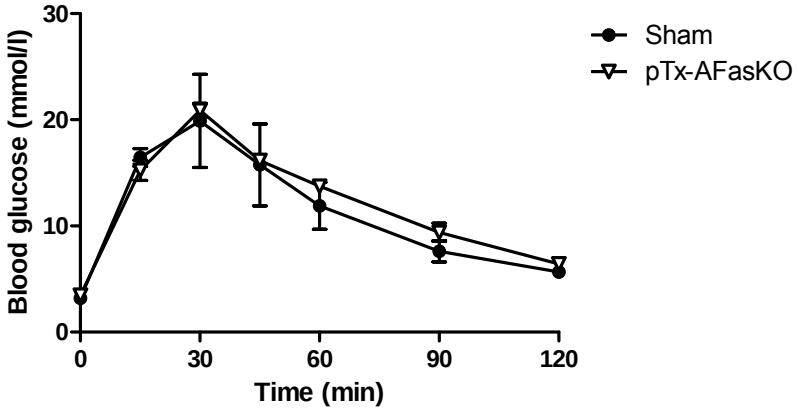

B

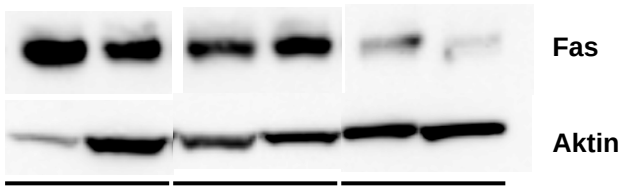

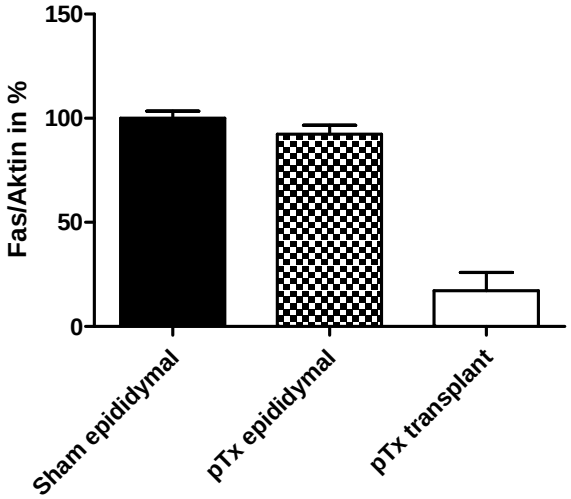

Fig. 11: Both epididymal fat pads were removed from a adipocyte-specific Fas-knockout mouse (donor; AFasKO) and stitched to the mesenterium of a wildtype mouse (recipient; pTx-AFasKO). (**A**) Intraperitoneal glucose tolerance test (2 g glucose/kg body weight) was performed four weeks after surgical procedure in mice receiving portal transplants (pTx-AFasKO; ∇) or in sham-operated mice (●). (**B**) Epididymal fat tissue of Sham-operated and portal transplanted mice as well as the portal transplant was collected and Fas was determined by Western blotting. Results are the mean ± SEM of 2-3 animals.

7.2 Impact of fat tissue transplantation on energy balance

Furthermore, weight of different endogenous fat pads was determined in mice receiving either a portal- or a caval-drained transplant. As shown in Fig. 12A "total" adipose tissue weight (sum of inguinal, epididymal, mesenteric and perinephric fat pads) was slightly decreased in caval-transplanted mice compared to portal-transplanted or sham-operated mice. This decrease was due to trend wise lower weights of epididymal, mesenteric and perinephric fat pads whereas weight of inguinal fat pads were similar in all three groups (Fig. 12B)

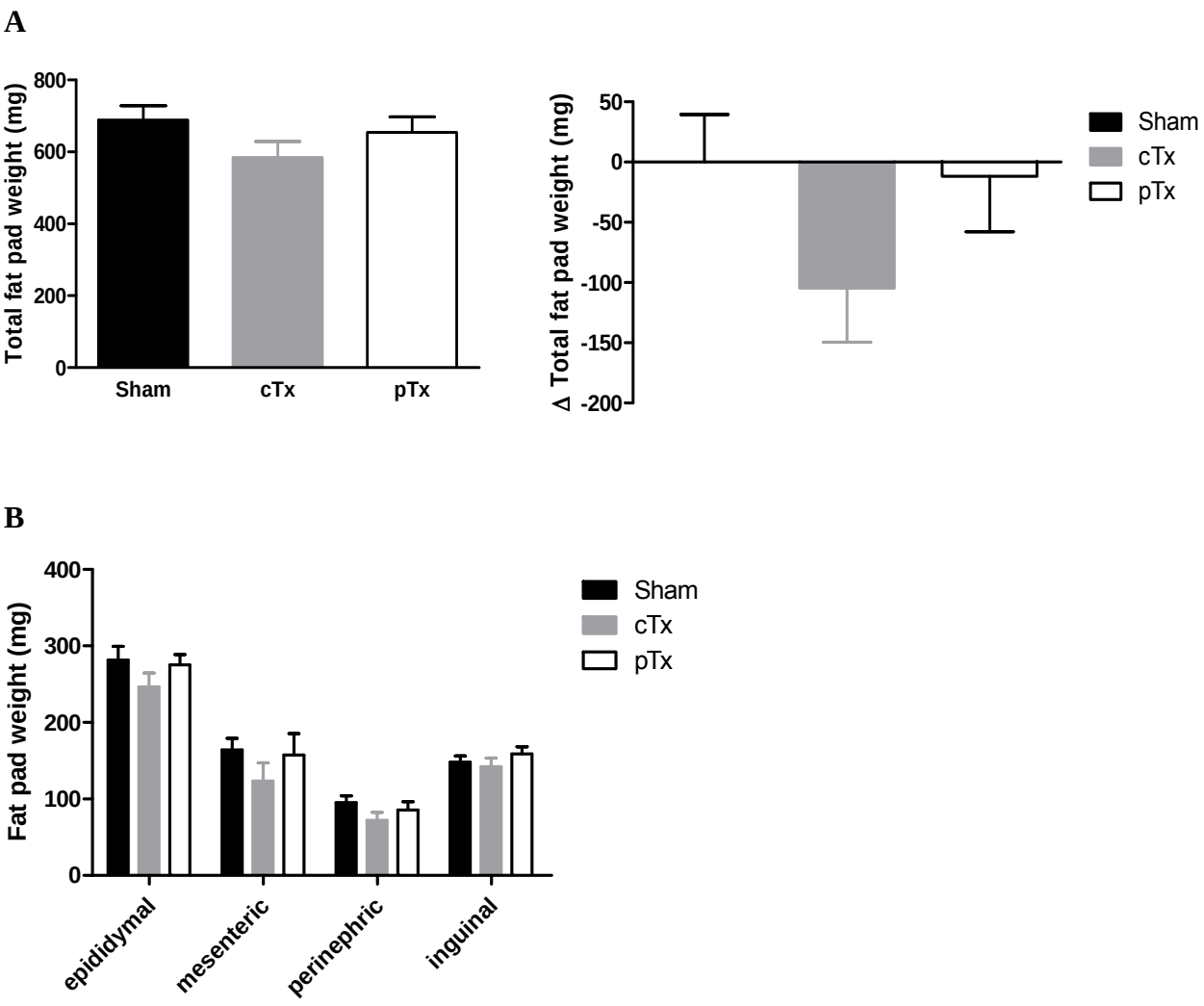

Fig. 12: (**A**) Endogenous fat pad mass was determined in portal, caval transplanted and sham-operated mice after 4 weeks of transplantation. (**B**) Total fat pad weight was determined for all groups (left panel) and calculated as a difference to sham-operated mice (right panel). Results are the mean of ± SEM 5-6 animals.

Given the above mentioned differences in fat pad weight between portal-transplanted, caval-transplanted and sham-operated mice we hypothesized that an artificial increase in fat mass by fat transplantation will impact on energy balance and that this effect is dependent on fat transplant localization. We therefore analyzed food intake, locomotor activity, energy expenditure and respiratory quotient in these mice using metabolic cages.

Food intake was measured hourly during light and dark phase for 24 hours. In Fig.13 the absolute food intake is shown for 24 hours. Food intake in mice is higher during dark phase than during light phase as they belong to nocturnal rodents. As depicted in Fig. 13B food intake during dark phase was similar in all three groups. However, portal and caval transplanted mice had an approximately 50 % higher intake during light phase compared to sham-operated mice (Fig. 13B). As a consequence, absolute food intake was slightly higher in portal-transplanted mice.

As depicted in Fig. 13A and Fig. 13B no apparent differences were found in energy expenditure and respiratory quotient between the three groups. However, mice receiving a portal-drained fat transplant showed an approx. 20% reduction in locomotor activity during the light phase (Fig. 14C).

A

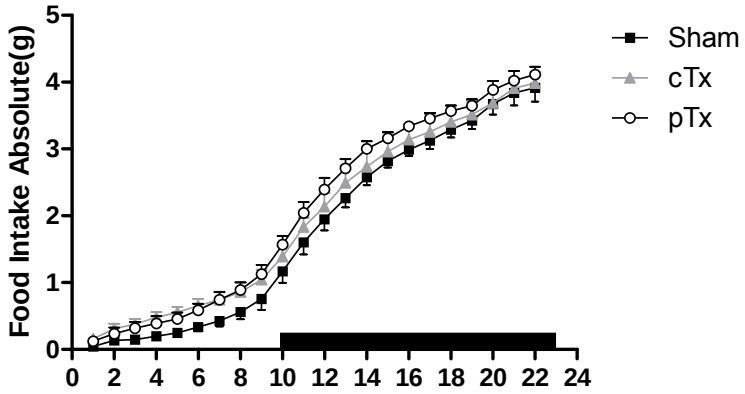

B

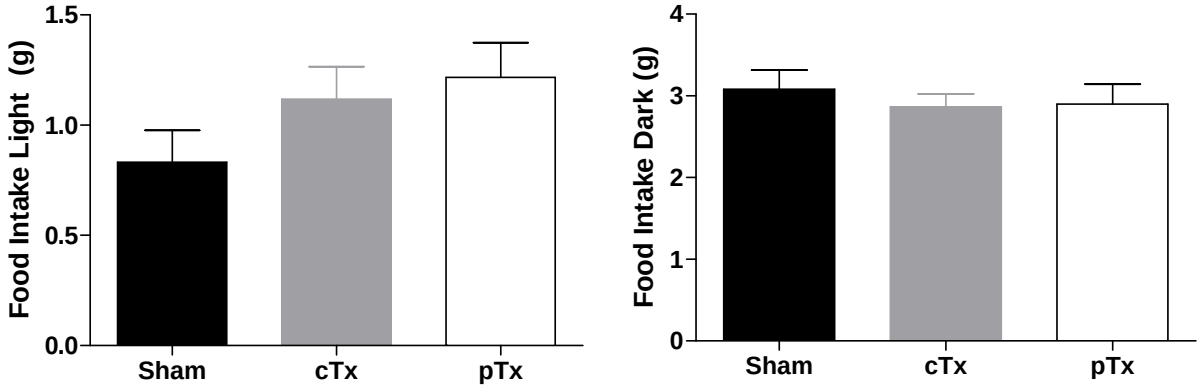

Fig. 13: (**A**) Absolute food intake of sham-operated, portal (pTx) and caval (cTx) transplanted mice was measured hourly during 24 h using metabolic cages. (**B**) Absolute food intake is shown in light and dark phase. Results are the mean of ± SEM 5-6 animals.

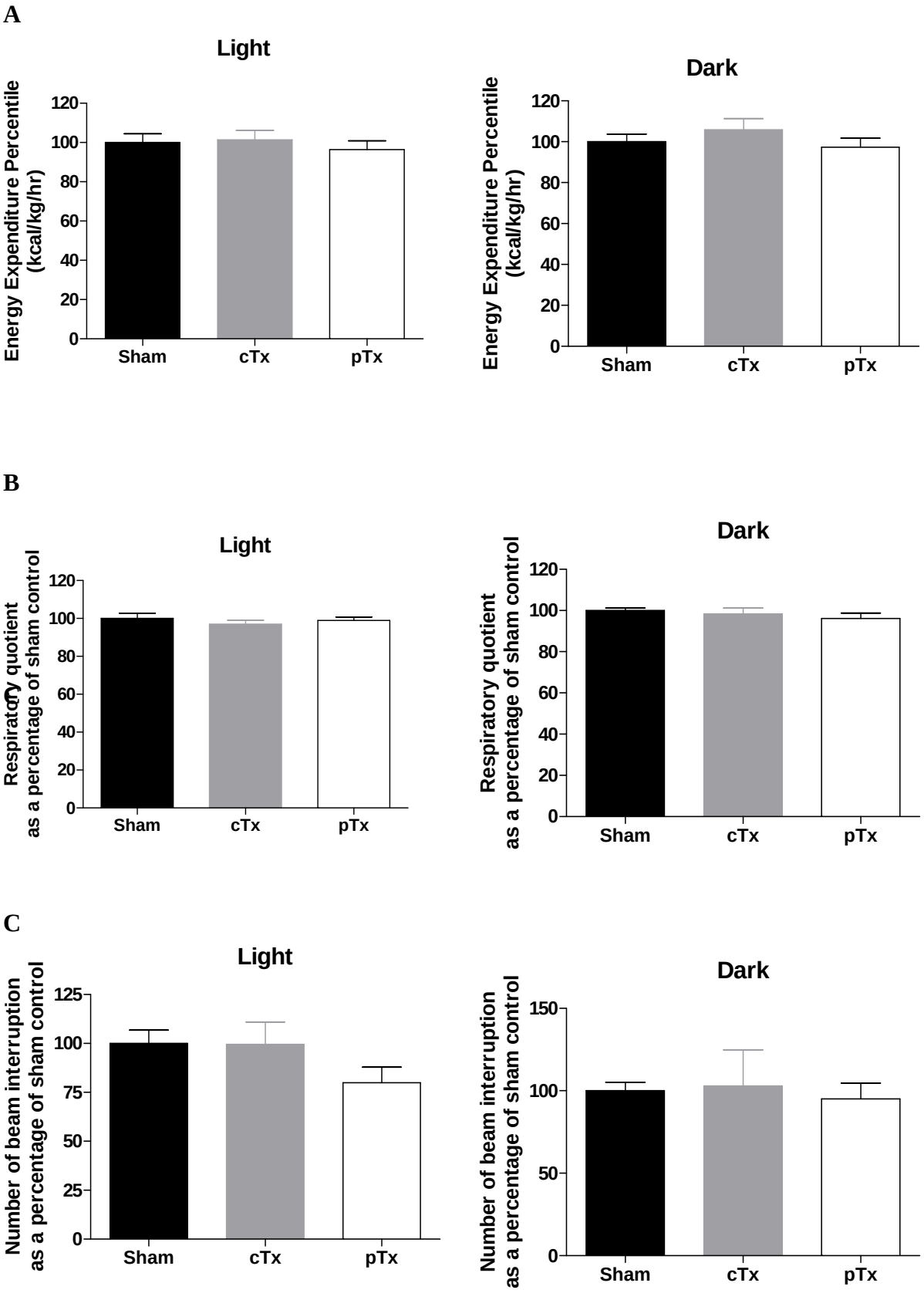

Fig. 14: Energy expenditure (**A**), respiratory quotient (**B**) and activity (**C**) were determined as percentile for light and dark phase of a 24 h measurement using metabolic cages. Results are the mean of ± SEM 5-6 animals.

In summary, mice receiving a portal-drained fat transplant show increased food intake and reduced locomotor activity during light phase, which might be responsible for the observed differences in fat mass and might impact on glucose homeostasis.

8 Discussion

8.1 The impact of fat tissue localization and its venous drainage on glucose homeostasis

The “portal hypothesis” proposes that the liver is directly exposed to free fatty acids and cytokines increasingly released from visceral fat tissue into the portal vein of obese subjects and, thus, rendering visceral fat accumulation particularly hazardous for the development of hepatic insulin resistance and type 2 diabetes (29-30). In this study, fat mass was depot-specifically, artificially increased utilizing a novel fat transplantation model. In accordance with the portal hypothesis, this study demonstrates that fat transplant localization impacts on glucose homeostasis through its venous drainage.

The metabolic relevance of specific fat depots, also their artificial increase by adipose tissue transplantation, has been discussed in previous studies (24, 31-33). In this context, the localization and especially the drainage of the described adipose tissue is often not clarified. Fat pads transplanted into intra-abdominal compartments have been described as visceral fat transplants, without making sure, that these pads are effectively drained into portal vein. Moreover, the origin and the amount of transplanted tissue vary in previous studies. However, in most of these studies epididymal fat pads were used as donor fat, as it was also the case in this study.

Besides fat pad origin, the importance of adipose tissue drainage has to be considered when effects on metabolism are determined. In an earlier study (24), glucose tolerance was improved in mice receiving a systemic drained transplant. These findings were confirmed by a more recent study from Hocking *et al*. (32). The aim of the present study was to develop a portal transplantation model mimicking visceral fat tissue accumulation. In contrast to mice receiving a systemically drained fat transplant, glucose tolerance was deteriorated in portal transplanted mice. Interestingly, Tran *et al*. found no changes in glucose tolerance in their model of intraabdominal fat pad transplantation. However, in contrast to our study, fat transplants in their study were drained both to the caval as well as to the portal vein. Similarly, we found here no alterations in glucose tolerance in mice receiving both a caval-drained as well as a portal-drained fat transplant (Fig. 4B). This is potentially due to the fact

that the beneficial metabolic effect of the caval drained fat transplant is balanced by the detrimental effect of the portal drained transplant.

Hepatic insulin resistance in mice receiving portal drained fat transplants corresponds with the conclusion of Miyazaki et al. (34) which postulates that visceral fat accumulation as opposed to subcutaneous fat accumulation is associated with hepatic insulin resistance. Interestingly, hepatic insulin resistance found in our study was not associated with hepatic steatosis or increased Kupffer cell activation (Fig. 8) as it was observed in high fat diet-induced hepatic insulin resistance (28, 35). These changes might be due to a direct effect of high fat diet on liver metabolism or due to an increased release of FFAs from visceral adipose tissue in high fat diet-fed mice. Accordingly, FFAs levels were not increased in mice receiving portal drained transplants.

Hepatic insulin resistance is often discussed in association with adipose tissue inflammation suggesting that activated macrophages produce pro-inflammatory cytokines such as IL-6 (15, 19-20). Moreover, chronic exposure to IL-6 inhibits hepatic insulin receptor signalling (18) and IL-6 activates the negative insulin signalling regulator SOCS-3 in C57BL/6J mice (20) implicating IL-6 as a contributor to the development of insulin resistance in obesity, particularly in the liver. Correspondingly, IL-6 expression in portal transplanted adipose tissue and IL-6 levels in the portal vein of mice receiving portal drained transplants were increased (Fig. 9A, B). Moreover, hepatic SOCS-3 expression was induced (Fig. 9C) and, consistently, insulin-stimulated Akt phosphorylation was reduced in the liver of these mice. This impairment of hepatic insulin signalling was not observed in mice receiving IL-6 deficient fat transplants (Fig. 9B). Hepatic SOCS-3 expression was accordingly not induced in those mice (Fig. 9D). Thus, these results point towards a causative role for IL-6 in the development of insulin resistance in portal transplanted mice.

Expression of pro-inflammatory cytokines, including IL-6, was increased in caval as well as portal transplanted fat pads (Fig. 9C). Remarkably, glucose metabolism was only deteriorated when transplants were drained to the portal vein. Moreover, portal transplantation of peritoneal tissue that did not contain adipose tissue had no effect on glucose tolerance (Fig. 4B). These data suggest that the transplantation procedure on its own does not deteriorate glucose homeostasis, for example, by altering the delivery of inflammatory mediators from the gastro-intestinal tract. Such finding emphasizes the importance of fat tissue localization and, thus, vascular drainage and indicates that the increased production of pro-inflammatory cytokines as it is found in obesity is particularly detrimental when released into the portal circulation supporting the portal hypothesis (30). Furthermore, besides IL-6 other factors may

have contributed to the deterioration of glucose tolerance and hepatic insulin resistance. Interestingly, lack of IL-6 also reduced expression of IL-1β in adipose tissue (Fig. 10C). Rotter *et al*. suggested that IL-6 induce insulin resistance in concert with other cytokines that are also upregulated in adipocytes (36). Especially IL-6 and IL-1β were shown to mediate the change of hepatic glucose metabolism, influencing the glucoregulatory action of insulin through their signal pathways involving protein phosphorylation (13, 37).

Interestingly, we found increased levels of FasL in portal transplanted fat pads. We previously reported that Fas activation by FasL-treatment induced secretion of IL-6 in 3T3-L1 adipocytes.(38). Conversely, adipocyte-specific Fas-knockout mice showed decreased IL-6 expression in adipose tissue and reduced circulating IL-6 levels (25). Thus, FasL-induced Fas-activation might be responsible for increased IL-6 secretion of portal transplanted fat pads ultimately inducing hepatic insulin resistance. Indeed, FasL expression was not reduced in portal transplanted IL-6 deficient fat pads suggesting that Fas-activation may be indeed upstream of IL-6 release (Fig. 10C). Furthermore, mice receiving fat transplants from AFasKO mice showed normal glucose tolerance. (Fig. 11A). Therefore, our results may suggest that Fas-activation may an important early step in the induction of pro-inflammatory cytokines in adipose tissue, e.g. in obesity.

8.2 Impact of fat tissue transplantation on energy balance

As depicted in Fig. 12B, endogenous mass of different fat pads was decreased in mice receiving a caval drained transplant whereas those pads of mice with portal drained transplants maintained almost the same fat mass as sham-operated mice. This suggests a self-regulatory process to maintain adipose tissue mass in caval transplanted but not in portal transplanted mice. We hypothesized that caval transplanted fat pads may secret a humoral factor that inhibits food intake and/or increases energy expenditure whereas portal transplanted fat pads do not secret such factor or the latter is removed during liver passage before reaching the brain. Thus, in collaboration with Prof. Thomas Lutz's group food intake and energy expenditure was analyzed.

Indeed, energy balance was affected by transplantation of additional adipose tissue. Particularly, mice with portal drained fat transplants had a slightly higher food intake than caval transplanted or sham-operated mice (Fig. 13A). Moreover, physical activity was

reduced only in mice receiving a portal transplant (Fig. 14C). Interestingly, several brain regions have been associated with energy homeostasis. At the molecular level, the melanocortin system plays a major role. Stimulation of proopiomelanocortin (POMC) neurons results finally in decreased food intake and increased energy expenditure (39-40). Leptin was previously shown to stimulate POMC neurons and hence, a reduction in circulating leptin levels lead to decreased stimulation of the POMC neurons resulting in higher food intake and decreased energy expenditure. So far, we have not found any differences in circulating leptin levels. However, leptin sensitivity may be different. Thus, we plan to analyze leptin signaling in the hypothalamus.

Mice are nocturnal animals, i.e. food intake is much higher during dark phase. Interestingly, increased food intake in mice receiving a fat transplant was due to increased food intake during light phase. In contrast, food intake during dark phase was not different from sham-operated or caval transplanted mice (Fig. 13B). As expected, sham-operated mice showed a normal food intake profile. Such finding may suggest alterations in circadian clock regulation. It has been suggested that changes in the metabolic state associated with obesity affect circadian rhythms with regard to activity, feeding and the cycling of clock genes and their downstream clock-controlled targets (41). Thus, our findings indicate that changes implemented by adipose tissue transplantation may alter the circadian clock depending on transplant localization. Ongoing projects in our laboratory will further evaluate the potential role of altered regulation in clock genes.

Using a novel adipose tissue transplantation paradigm we demonstrate that portal delivery of cytokines such as IL-6 induces hepatic insulin resistance and impacts on energy homeostasis. Thus, we provide further evidence for the "portal hypothesis", which explains the strong association between visceral fat accumulation and (hepatic) insulin resistance by increased drainage of pro-inflammatory cytokines and lipids to the portal vein.

9 Acknowledgements

I would like to thank my supervisor PD Dr. Daniel Konrad for giving me the opportunity to do the PhD in his lab. I am grateful for his efficient and straight supervision during my thesis and for his fair-minded attitude. The work in this lab with my lab colleagues Stephan Wüest and Reto Rapold was always a pleasure and I am thankful for the experience and patience I learned during this work. I also would like to thank Prof. Dr. Eugen Schoenle for his helpful and constructive support.

I would like to thank my thesis committee members, Prof. Dr. Marc Donath, Prof. Dr. Carsten Wagner, Prof. Dr. Thomas Lutz and Prof. Dr. Emanuel Christ. Many thanks also to Dr. Assaf Rudich.

I would like to thank Dr. Maggy Arras and Christina Boyle for their technical help regarding animal experiments.

In particular, I thank all the people in the C Lab for their help and pleasant time during my work. Especially the mental support and motivating discussions with the C Lab 41 are unforgettable and of inestimable value. Thank you: Daniel, Lin, Simone, Francesca and Marcela.

Special thanks go to my boyfriend Christian who was always a great motivating help during this time. Thank you for listening and your support. I thank all my friends who attended me during my thesis for enjoying the other bride sites of life. And above all, I would like to thank my whole family who encouraged me during my long education.

10 References

1. Yach, D., Stuckler, D., and Brownell, K.D. 2006. Epidemiologic and economic consequences of the global epidemics of obesity and diabetes. *Nat Med* 12:62-66.
2. Kopelman, P.G. 2000. Obesity as a medical problem. *Nature* 404:635-643.
3. Willett, W.C., Dietz, W.H., and Colditz, G.A. 1999. Guidelines for healthy weight. *N Engl J Med* 341:427-434.
4. Wild, S., Roglic, G., Green, A., Sicree, R., and King, H. 2004. Global prevalence of diabetes: estimates for the year 2000 and projections for 2030. *Diabetes Care* 27:1047-1053.
5. Stumvoll, M., Goldstein, B.J., and van Haeften, T.W. 2008. Type 2 diabetes: pathogenesis and treatment. *Lancet* 371:2153-2156.
6. Bergman, R.N. 1989. Lilly lecture 1989. Toward physiological understanding of glucose tolerance. Minimal-model approach. *Diabetes* 38:1512-1527.
7. Senn, J.J., Klover, P.J., Nowak, I.A., Zimmers, T.A., Koniaris, L.G., Furlanetto, R.W., and Mooney, R.A. 2003. Suppressor of cytokine signaling-3 (SOCS-3), a potential mediator of interleukin-6-dependent insulin resistance in hepatocytes. *J Biol Chem* 278:13740-13746.
8. Vazquez-Vela, M.E., Torres, N., and Tovar, A.R. 2008. White adipose tissue as endocrine organ and its role in obesity. *Arch Med Res* 39:715-728.
9. Lord, G.M., Matarese, G., Howard, J.K., Baker, R.J., Bloom, S.R., and Lechler, R.I. 1998. Leptin modulates the T-cell immune response and reverses starvation-induced immunosuppression. *Nature* 394:897-901.
10. Elmquist, J.K. 2001. Hypothalamic pathways underlying the endocrine, autonomic, and behavioral effects of leptin. *Int J Obes Relat Metab Disord* 25 Suppl 5:S78-82.
11. Frayn, K.N. 2000. Visceral fat and insulin resistance--causative or correlative? *Br J Nutr* 83 Suppl 1:S71-77.
12. Fried, S.K., Russell, C.D., Grauso, N.L., and Brolin, R.E. 1993. Lipoprotein lipase regulation by insulin and glucocorticoid in subcutaneous and omental adipose tissues of obese women and men. *J Clin Invest* 92:2191-2198.
13. Shoelson, S.E., Lee, J., and Goldfine, A.B. 2006. Inflammation and insulin resistance. *J Clin Invest* 116:1793-1801.
14. Yang, X., and Smith, U. 2007. Adipose tissue distribution and risk of metabolic disease: does thiazolidinedione-induced adipose tissue redistribution provide a clue to the answer? *Diabetologia* 50:1127-1139.
15. Carey, A.L., and Febbraio, M.A. 2004. Interleukin-6 and insulin sensitivity: friend or foe? *Diabetologia* 47:1135-1142.
16. Weisberg, S.P., McCann, D., Desai, M., Rosenbaum, M., Leibel, R.L., and Ferrante, A.W., Jr. 2003. Obesity is associated with macrophage accumulation in adipose tissue. *J Clin Invest* 112:1796-1808.
17. Oakes, N.D., Cooney, G.J., Camilleri, S., Chisholm, D.J., and Kraegen, E.W. 1997. Mechanisms of liver and muscle insulin resistance induced by chronic high-fat feeding. *Diabetes* 46:1768-1774.
18. Klover, P.J., Zimmers, T.A., Koniaris, L.G., and Mooney, R.A. 2003. Chronic exposure to interleukin-6 causes hepatic insulin resistance in mice. *Diabetes* 52:2784-2789.
19. Ogawa, W., and Kasuga, M. 2008. Cell signaling. Fat stress and liver resistance. *Science* 322:1483-1484.

20. Sabio, G., Das, M., Mora, A., Zhang, Z., Jun, J.Y., Ko, H.J., Barrett, T., Kim, J.K., and Davis, R.J. 2008. A stress signaling pathway in adipose tissue regulates hepatic insulin resistance. *Science* 322:1539-1543.
21. Wueest, S., Rapold, R.A., Schumann, D.M., Rytka, J.M., Schildknecht, A., Nov, O., Chervonsky, A.V., Rudich, A., Schoenle, E.J., Donath, M.Y., et al. Deletion of Fas in adipocytes relieves adipose tissue inflammation and hepatic manifestations of obesity in mice. *J Clin Invest* 120:191-202.
22. Ayala, J.E., Bracy, D.P., McGuinness, O.P., and Wasserman, D.H. 2006. Considerations in the design of hyperinsulinemic-euglycemic clamps in the conscious mouse. *Diabetes* 55:390-397.
23. Fisher, S.J., and Kahn, C.R. 2003. Insulin signaling is required for insulin's direct and indirect action on hepatic glucose production. *J Clin Invest* 111:463-468.
24. Konrad, D., Rudich, A., and Schoenle, E.J. 2007. Improved glucose tolerance in mice receiving intraperitoneal transplantation of normal fat tissue. *Diabetologia* 50:833-839.
25. Wueest, S., Rapold, R.A., Schumann, D.M., Rytka, J.M., Schildknecht, A., Nov, O., Chervonsky, A.V., Rudich, A., Schoenle, E.J., Donath, M.Y., et al. 2010. Deletion of Fas in adipocytes relieves adipose tissue inflammation and hepatic manifestations of obesity in mice. *J Clin Invest* 120:191-202.
26. Pfaffl, M.W. 2001. A new mathematical model for relative quantification in real-time RT-PCR. *Nucleic Acids Res* 29:e45.
27. Weir, J.B. 1990. New methods for calculating metabolic rate with special reference to protein metabolism. 1949. *Nutrition* 6:213-221.
28. Huang, W., Metlakunta, A., Dedousis, N., Zhang, P., Sipula, I., Dube, J.J., Scott, D.K., and O'Doherty, R.M. 2010. Depletion of liver Kupffer cells prevents the development of diet-induced hepatic steatosis and insulin resistance. *Diabetes* 59:347-357.
29. Bjorntorp, P. 1990. "Portal" adipose tissue as a generator of risk factors for cardiovascular disease and diabetes. *Arteriosclerosis* 10:493-496.
30. Kabir, M., Catalano, K.J., Ananthnarayan, S., Kim, S.P., Van Citters, G.W., Dea, M.K., and Bergman, R.N. 2005. Molecular evidence supporting the portal theory: a causative link between visceral adiposity and hepatic insulin resistance. *Am J Physiol Endocrinol Metab* 288:E454-461.
31. Tran, T.T., Yamamoto, Y., Gesta, S., and Kahn, C.R. 2008. Beneficial effects of subcutaneous fat transplantation on metabolism. *Cell Metab* 7:410-420.
32. Hocking, S.L., Chisholm, D.J., and James, D.E. 2008. Studies of regional adipose transplantation reveal a unique and beneficial interaction between subcutaneous adipose tissue and the intra-abdominal compartment. *Diabetologia* 51:900-902.
33. Gavrilova, O., Marcus-Samuels, B., Graham, D., Kim, J.K., Shulman, G.I., Castle, A.L., Vinson, C., Eckhaus, M., and Reitman, M.L. 2000. Surgical implantation of adipose tissue reverses diabetes in lipoatrophic mice. *J Clin Invest* 105:271-278.
34. Miyazaki, Y., and DeFronzo, R.A. 2009. Visceral fat dominant distribution in male type 2 diabetic patients is closely related to hepatic insulin resistance, irrespective of body type. *Cardiovasc Diabetol* 8:44.
35. Lanthier, N., Molendi-Coste, O., Horsmans, Y., van Rooijen, N., Cani, P.D., and Leclercq, I.A. 2009. Kupffer cell activation is a causal factor for hepatic insulin resistance. *Am J Physiol Gastrointest Liver Physiol*.
36. Rotter, V., Nagaev, I., and Smith, U. 2003. Interleukin-6 (IL-6) induces insulin resistance in 3T3-L1 adipocytes and is, like IL-8 and tumor necrosis factor-alpha, overexpressed in human fat cells from insulin-resistant subjects. *J Biol Chem* 278:45777-45784.

37. Kanemaki, T., Kitade, H., Kaibori, M., Sakitani, K., Hiramatsu, Y., Kamiyama, Y., Ito, S., and Okumura, T. 1998. Interleukin 1beta and interleukin 6, but not tumor necrosis factor alpha, inhibit insulin-stimulated glycogen synthesis in rat hepatocytes. *Hepatology* 27:1296-1303.
38. Wueest, S., Rapold, R.A., Rytka, J.M., Schoenle, E.J., and Konrad, D. 2009. Basal lipolysis, not the degree of insulin resistance, differentiates large from small isolated adipocytes in high-fat fed mice. *Diabetologia* 52:541-546.
39. Froy, O. 2010. Metabolism and circadian rhythms--implications for obesity. *Endocr Rev* 31:1-24.
40. Cone, R.D. 2005. Anatomy and regulation of the central melanocortin system. *Nat Neurosci* 8:571-578.
41. Kohsaka, A., Laposky, A.D., Ramsey, K.M., Estrada, C., Joshu, C., Kobayashi, Y., Turek, F.W., and Bass, J. 2007. High-fat diet disrupts behavioral and molecular circadian rhythms in mice. *Cell Metab* 6:414-421.

11 Curriculum Vitae

Personal Data

Last name:	RYTKA
First name:	Julia
Date of birth:	May, 5th, 1980
Nationality:	German

Education

Since 07/ 2007	PhD at the University of Zürich, Childrens Hospital "The impact of adipose tissue drainage on glucose homeostasis" Part of the Integrative Molecular Medicine (imMed) PhD program of the Zurich Center of Human Physiology (ZIHP), University of Zürich
09/ 2001- 01/ 2007	Diploma in Nutrition Sciences at the University of Potsdam, Germany (Diplom Ernährungswissenschaft)
07/ 2006 - 01/ 2007	Diploma thesis at ETH Zürich, Switzerland Laboratory of Food Biotechnology Institute of Food Science and Nutrition "New in vitro colonic fermentation model for Salmonella infection in the child gut"(1)
10/ 2000 - 09/ 2001	Studies in Biology at the University of Würzburg, Germany
09/ 1991- 06/2000	Matura at „Deutschhaus-Gymnasium", Würzburg, Germany

Oral Presentations

06/ 2010	Schweizer Gesellschaft für Pädiatrie, Crans Montana, Switzerland
08/2010	6th Symposium of the Zentrum für intergrative Humanphysiologie (ZIHP), University of Zürich
09/ 2010	46th Annual meeting of the European Association of the Study of Diabetes (EASD), Stockholm, Sweden

Publications

1 **Rytka J***, Le Blay G*, Zihler A, Lacroix C. New in vitro colonic fermentation model for Salmonella infection in the child gut. *FEMS Microbiol Ecol* 2009; 67(2):198-207.

* *shared first authorship*

2 Wueest S, Rapold RA, **Rytka JM**, Schoenle EJ, Konrad D. Basal biolysis, not the degree of insulin resistance, differentiates large from small isolated adipocytes in high-fat fed mice. *Diabetologia* 2009; 52(3): 541-546

3 Wueest, S., Rapold, R.A., Schumann, D.M., **Rytka, J.M**., Schildknecht, A., Nov, O., Chervonsky, A.V., Rudich, A., Schoenle, E.J., Donath, M.Y., et al. Deletion of Fas in adipocytes relieves adipose tissue inflammation and hepatic manifestations of obesity in mice. *J Clin Invest* 120:191-202.

4 J.A. Ehses, D.T. Meier, S. Wueest, **J. Rytka**, S. Boller, P.Y. Wielinga, A. Schraenen, K. Lemaire, S. Debray, L.Van Lommel, J.A. Pospisilik, O. Tschopp, S.S. Manuel, U. Malipiero, H. Esterbauer, H. Ellingsgaard, S. Rütti, F.C. Schuit, T.A. Lutz, M. Böni-Schnetzler, D. Konrad, Marc Y. Donath Toll-like receptor 2 deficient mice are protected from high fat diet-induced insulin resistance and beta cell dysfunction *Diabetologia* 53:1795-1806

5 **Julia M. Rytka**, Stephan Wueest, Eugen J. Schoenle, Daniel Konrad The metabolic consequences of abdominal fat tissue transplantation are determined by the transplant's venous drainage and portal interleukin-6 levels (under revision)